

# 1 A critical reappraisal of paleomagnetic evidence for Philippine Sea 2 Plate rotation

3

4 Suzanna H.A. van de Lagemaat<sup>1,\*</sup>, Daniel Pastor-Galán<sup>2,3</sup>, Bas B.G. Zanderink<sup>1</sup>, Maria J.Z. Villareal<sup>4</sup>,  
5 John W. Jenson<sup>4</sup>, Mark J. Dekkers<sup>1</sup>, Douwe J.J. van Hinsbergen<sup>1</sup>

6

7 \*Corresponding author: Suzanna van de Lagemaat (s.h.a.vandelagemaat@uu.nl)

8

9 <sup>1</sup>Department of Earth Sciences, Utrecht University, the Netherlands

10 <sup>2</sup>Department of Geodynamics, Universidad de Granada, Spain

11 <sup>3</sup>Frontier Research Institute for Interdisciplinary Sciences, Tohoku University, Japan

12 <sup>4</sup>Water Environmental Research Institute of the Western Pacific, University of Guam, USA

13

## 14 **Highlights:**

- 15 - New paleomagnetic data from Eocene, Oligocene, and Miocene locations in Guam
- 16 - Reassessment of published paleomagnetic data using recent quality criteria
- 17 - Paleomagnetic data do not unequivocally demonstrate whole-plate vertical-axis rotation
- 18 - Northward motion of the Philippine Sea Plate since the mid-Eocene was about 15°

19

20 **Keywords:** Paleomagnetism; Guam; Philippine Sea Plate; Philippines; Philippine Mobile Belt; Izu-  
21 Bonin Mariana

22

23 **This is a non-peer reviewed manuscript submitted to EarthArxiv. The manuscript has been**  
24 **submitted for peer-review to *Tectonophysics***

25 **Abstract**

26 The kinematic history of the Philippine Sea Plate (PSP) is crucial for interpreting its geological  
27 record related to subduction initiation processes and the paleogeography of the junction between  
28 the Paleo-Pacific and Tethyan oceanic realms. However, reconstructing PSP's kinematic history is  
29 difficult because the plate has been surrounded by subduction zones for most of its history. In  
30 absence of marine magnetic anomalies to constrain PSP's motion relative to its neighboring plates,  
31 paleomagnetic data may be used as quantitative constraints on its motion. Previous paleomagnetic  
32 studies interpreted easterly deflected declinations to infer clockwise rotations of up to 90° since the  
33 Eocene. However, rotations inferred from these datasets may also reflect local block rotations related  
34 to plate margin deformation. We here re-evaluate to what extent paleomagnetic data from the PSP  
35 unequivocally demonstrate plate motion rather than local rotation. To this end, we provide new data  
36 from Guam, in the Mariana forearc, and reassess published paleomagnetic data. Our new data from  
37 Guam come from two localities in the Eocene, two in the Oligocene, and two in the Miocene. Our  
38 compilation assesses data quality against recently defined criteria. Our new results demonstrate that  
39 in Guam, local rotation differences of up to 35° occurred since the Eocene. Our compilation identifies  
40 both clockwise and counterclockwise rotations from the plate margins, with little confidence which  
41 of these would reflect plate-wide rotation. We compiled paleolatitude data from igneous rocks, which  
42 we correct for microplate rotation constrained by intra-PSP marine magnetic anomalies and show a  
43 northward drift of the PSP of ~15° since the Eocene, but without a paleomagnetic necessity for  
44 major vertical axis rotation. Hence, with the currently available data, reconstructing rotations may be  
45 permitted, but are not required. Plate motion is currently better reconstructed from geological  
46 constraints contained in circum-PSP orogenic belts.

47

48

49 **1. Introduction**

50 For most of its tectonic history since the Eocene, the Philippine Sea Plate (PSP) and associated  
51 microplates have been surrounded by subduction zones (e.g., Hall, 2002; Gaina and Müller, 2007; Wu  
52 et al., 2016). Consequently, the reconstruction of the PSP relative to the surrounding major plates of  
53 the Pacific, Australia, and Eurasia cannot be determined from marine magnetic anomalies, and  
54 reconstruction of its past tectonic motions is challenging. In such cases, paleomagnetic data may  
55 provide quantitative constraints on paleolatitude evolution and vertical axis rotation of the plate  
56 (e.g., Fuller et al., 1989; Haston and Fuller, 1991; Hall et al., 1995a, 1995b), which may then be  
57 incorporated in reconstructions based on geological (e.g., Hall, 2002) or seismic tomographic data  
58 (Wu et al., 2016).

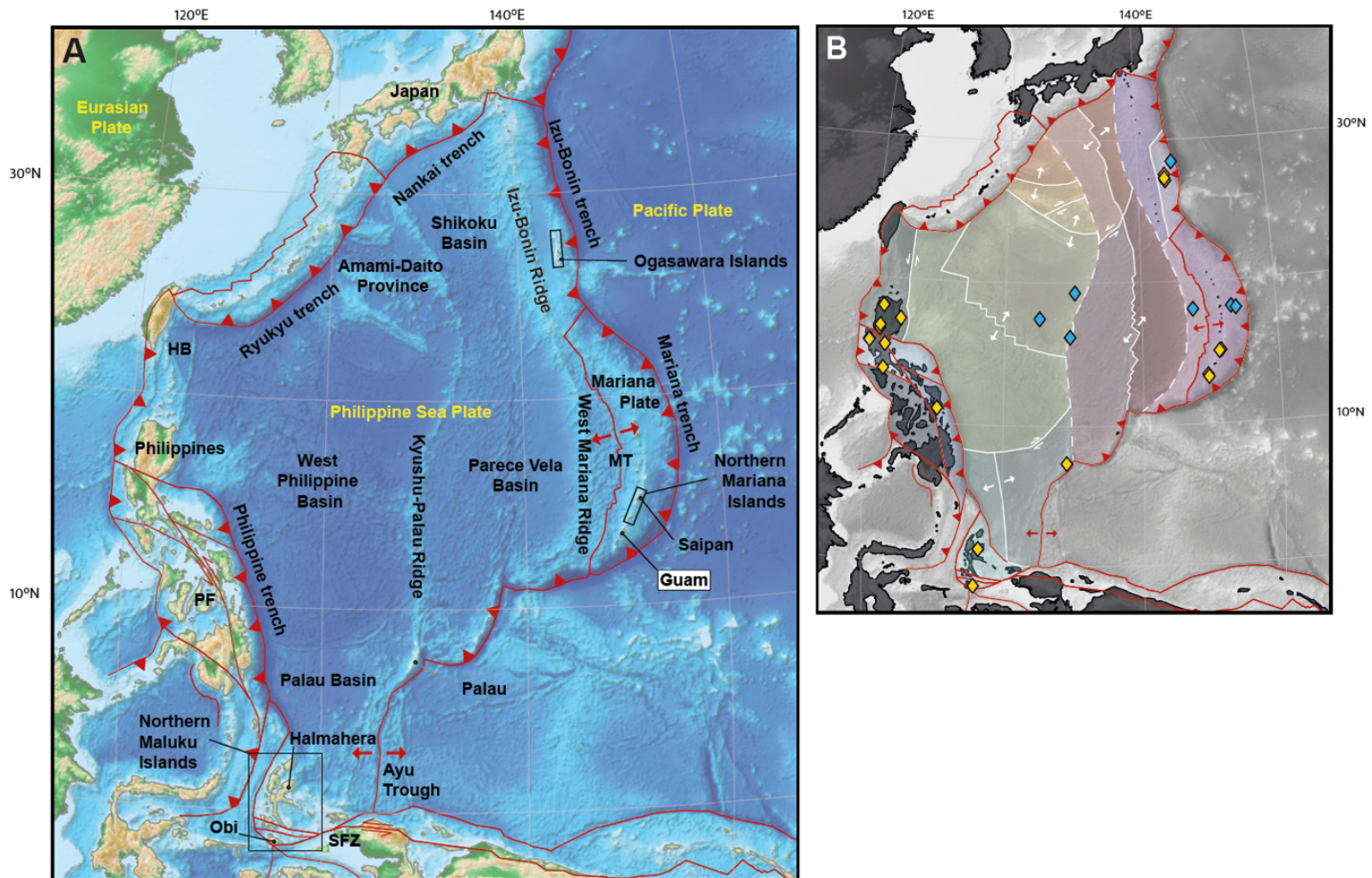
59 The paleomagnetic data from the PSP come from rocks exposed on the plate margins (Fig. 1),  
60 i.e., on the Philippines and Halmahera in the west and the islands in the arc and forearc adjacent to  
61 the Marianas and Izu-Bonin trenches in the east, as well as from boreholes in the plate interior. Even  
62 though the database is extensive (e.g., Loudon, 1977; Kinoshita, 1980; Keating and Herrero, 1980;

63 Keating, 1980; Bleil, 1982; Fuller et al., 1989; Haston and Fuller, 1991; Haston et al., 1992; Koyama et  
64 al., 1992; Hall et al., 1995a, b; Queaño et al., 2007, 2009; Yamazaki et al., 2010, 2021; Balmater et al.,  
65 2015; Richter and Ali, 2015; Liu et al., 2021; Sager and Carvallo, 2022), these sampling locations  
66 come with challenges in providing firm constraints on plate motion evolution. The western plate  
67 margin is strongly deformed by distributed strike-slip faults and thrusts which makes it difficult to  
68 assess whether vertical axis rotations are local or plate-wide (e.g., Queaño et al., 2007). The eastern  
69 plate margin is also strongly deformed, e.g., by extensional processes opening forearc and back-arc  
70 basins (e.g., Yamazaki et al., 2003; Sdrolias et al., 2004). The drill cores in the plate's interior yielded  
71 large paleomagnetic datasets (e.g., Loudon, 1977; Kinoshita et al., 1980; Keating and Herrero, 1980;  
72 Keating, 1980; Bleil, 1982; Yamazaki et al., 2010, 2021; Richter and Ali, 2015; Sager and Carvallo,  
73 2022), but these are not azimuthally oriented and can only be used to constrain paleolatitude. As a  
74 result, declinations from the PSP vary widely and it is difficult to establish whether declination data  
75 may be interpreted as representative for rotation of the PSP in its entirety, and which represent local  
76 block rotations of the deformed plate margins. Despite the ambiguity in paleomagnetic data  
77 interpretation, most models include major clockwise rotation of up to 90° of the PSP, following  
78 paleomagnetic constraints (e.g., Haston and Fuller, 1991; Hall et al., 1995a; Deschamps and  
79 Lallemand, 2002; Sdrolias et al., 2004; Seton et al., 2012; Wu et al., 2016; Liu et al., 2023), sometimes  
80 despite questioning the reliability of paleomagnetic data (Wu et al., 2016). Others chose to not use  
81 paleomagnetic data as unput for their reinstruction (e.g., Xu et al., 2014), or only to a limited extent  
82 (Zahirovic et al., 2014), and therefore those reconstructions include a much smaller rotation or no  
83 vertical-axis rotation at all.

84 While declination data of the PSP may be considered as ambiguous, paleomagnetic studies to  
85 obtain inclination data are still useful, as they provide insight into the paleolatitude evolution of the  
86 PSP. Published paleomagnetic data are often indicating Eocene paleolatitudes that are about 20°  
87 lower than today (e.g., Haston and Fuller, 1991; Hall et al., 1995b; Queaño et al., 2007; Yamazaki et  
88 al., 2010), although paleolatitudes obtained from sediments are subject to inclination shallowing.  
89 Taking the relative motions of the present and former microplates that together comprise the PSP  
90 into account that are reconstructed from marine magnetic anomalies (Hilde and Lee, 1984;  
91 Deschamps and Lallemand, 2002; Yamazaki et al., 2003; Sdrolias et al., 2004), these paleolatitudes  
92 provide valuable information on PSP motions.

93 In this paper, we compile the current state-of-the art of the paleomagnetic database of the  
94 PSP and surrounding former and present microplates, and re-evaluate the paleomagnetic evidence  
95 for major vertical-axis plate rotation. We report newly collected paleomagnetic data from the island  
96 of Guam, located in the forearc of the southernmost portion of the Izu-Bonin Mariana (IBM)  
97 subduction zone, whose crust formed shortly after initiation of the present subduction zone in the  
98 Eocene (Ishizuka et al., 2011a, 2018; Reagan et al., 2010, 2013, 2019; Hickey-Vargas et al., 2018). We  
99 collected samples from Eocene, Oligocene, and Miocene volcanic and sedimentary rocks from Guam,  
100 whereby we collected samples from two localities of each epoch to evaluate whether declinations are

101 coherent on the scale of the island. We add these data to our compilation of previously published  
102 paleomagnetic data from the PSP. We evaluate the reliability of the available paleolatitude  
103 constraints using recently defined quality criteria (Meert et al., 2020; Vaes et al., 2021; Gerritsen et  
104 al., 2022). We will use these to critically re-evaluate the paleomagnetic constraints on vertical-axis  
105 rotation and paleolatitudinal evolution of the PSP.



106 **Figure 1:** A) Geographic map of the Philippine Sea Plate region; B) Current and former microplates of  
107 the PSP. Current plate boundaries (based on Bird, 2003) in red, former plate boundaries in white. Yellow  
108 (blue) diamonds on panel B mark sampling locations of previously published paleomagnetic data  
109 obtained from igneous rocks in field (borehole) localities. Base map is ETOPO 2022 15 Arc-Second  
110 Global Relief Model (NOAA National Centers for Environmental Information, 2022). HB: Huatung Basin;  
111 MT: Mariana Trough; PF: Philippine Fault; SFZ: Sorong Fault Zone

112

## 113 2. Geological setting

114 The PSP is in the West Pacific realm and is separated from the Pacific Plate by the Izu-Bonin Mariana  
115 subduction zone, where the Pacific Plate is subducting westwards below the PSP (Fig. 1). The PSP  
116 contains small remains of Jurassic and Cretaceous ocean floor and arc sequences (e.g., Dimalanta et  
117 al., 2020; Yumul et al., 2020; Ishizuka et al., 2022, and references therein), as well as several inactive

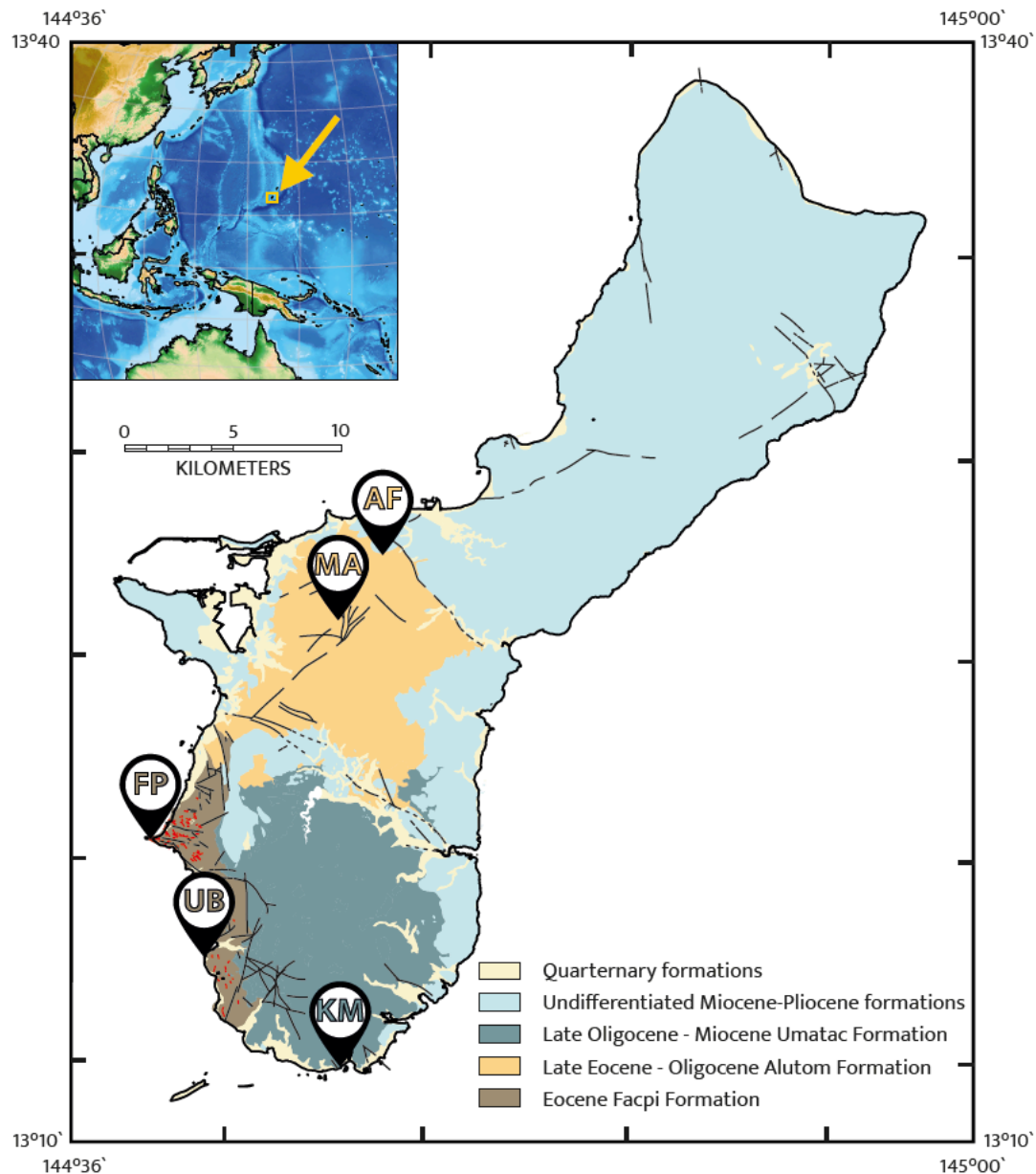
118 spreading ridges where the plate's lithosphere grew at different times throughout much of the  
119 Cenozoic (Hilde and Lee, 1984; Deschamps and Lallemand, 2002; Sdrolias et al., 2004). At present,  
120 one microplate (the Mariana microplate carrying the Mariana arc, including Guam) is diverging from  
121 the PSP, accommodated by oceanic spreading in the Mariana Trough (Fig. 1). This separated the  
122 active arc from the now inactive West Mariana Ridge, a remnant volcanic arc that was active until the  
123 Miocene (e.g., Yamazaki et al., 2003). To the north, the Mariana Trough spreading center disappears  
124 and no oceanic spreading is currently active in the Izu-Bonin ridge region (Fig. 1). The Izu-Bonin  
125 Ridge and West Mariana Ridge remnant arcs form the eastern margin of the Shikoku-Parece Vela  
126 Basin that hosts former oceanic spreading centers that were simultaneously active in the Oligocene-  
127 Miocene (c. 30-15 Ma; Sdrolias et al., 2004; Ishizuka et al., 2010), although different kinematic  
128 solutions have been proposed for the formation of each basin (Sdrolias et al., 2004). The western  
129 boundary of the Shikoku-Parece Vela Basin is the Kyushu-Palau Ridge, another remnant volcanic arc  
130 with magmatic rocks that formed from c. 48 to 25 Ma (Ishizuka et al., 2011b). To the west of the  
131 Kyushu-Palau Ridge is the West Philippine Basin (Fig. 1). This basin hosts a fossil spreading center  
132 that formed through N-S spreading (in present-day coordinates), between ~54 and 34 Ma (Hilde and  
133 Lee, 1984; Deschamps and Lallemand, 2002). In the north, in the Amamii-Daito Province, the PSP  
134 hosts a series of Cretaceous remnant arcs with intervening basins (e.g., Hickey-Vargas, 2005;  
135 Ishizuka et al., 2022; Hickey-Vargas et al., 2013; Morishita et al., 2018). Based on radiometrically  
136 dated dredged and drilled samples, it was interpreted that these basins opened in the Eocene,  
137 between c. 52 and 42 Ma (Hickey-Vargas, 1998; Ishizuka et al., 2013, 2018, 2022). The formation  
138 history of the different basins of the PSP thus indicates that the plate is a composite of about a dozen  
139 lithospheric fragments that formed at spreading centers in different orientations and at different  
140 times since ~54 Ma, within a Jurassic and Cretaceous lithosphere overlain by Cretaceous arc rocks.

141 Guam is the southernmost island exposed on the Mariana Ridge (Fig. 1). Together with the  
142 Northern Mariana Islands (Rota, Tinian, and Saipan), it forms the subaerially exposed forearc of the  
143 Mariana subduction zone. The currently active Mariana arc is located to the west and north of Guam  
144 and the Northern Mariana Islands. Guam exposes a stratigraphy spanning the Eocene to the  
145 Quaternary (Fig. 2). The northern half of Guam is dominated by Neogene limestone formations,  
146 which are also exposed in a smaller area in the southeast of the island (Fig. 2). The southern half of  
147 the island exposes Eocene to Miocene volcanics, volcanoclastic sediments, and minor limestones (Fig.  
148 2). The oldest rocks exposed on Guam, dated to  $43.8 \pm 1.6$  Ma using K-Ar whole-rock dating (Meijer et  
149 al., 1983), form the Eocene Facpi Formation, which comprises pillow basalts and andesite flows  
150 thought to have formed on the flanks of a strata-volcano (Reagan and Meijer, 1984; Siegrist and  
151 Reagan, 2008). The Facpi Formation is exposed in the southwest of the island, with fresh outcrops  
152 along the coastline. Apart from a small eastward tilt, there is no coherent structure within the pillow  
153 basalts, but the orientation of (sub)vertical dikes is predominantly NW-SE to roughly E-W. The Facpi  
154 Formation is cut by steeply dipping normal faults with similar orientations as the dikes (Reagan and  
155 Meijer, 1984; Siegrist and Reagan, 2008). Such normal faults do not occur in Miocene and younger

156 formations, which suggests that they may have formed shortly after or during eruption of the Facpi  
157 Formation volcanics (Reagan and Meijer, 1984). Because of these faults, we interpret the 10-30°  
158 bedding tilts of the pillow basalts resulting from deformation.

159         The Eocene pillow basalts and dikes are overlain by Eocene-Oligocene sediments of the  
160 Alutom Formation, which comprises mostly volcanoclastics, including bedded breccias,  
161 conglomerates, turbiditic sandstones, and minor limestone (Reagan and Meijer, 1984; Siegrist and  
162 Reagan, 2008). It is exposed in the northern part of the southern half of island, to the north of the  
163 Facpi Formation. The Alutom formation is late Eocene to earliest most Oligocene as shown by the  
164 occurrence of late Eocene foraminifera in its base section(Tracey et al., 1964) and K-Ar whole rock  
165 ages between 35.6±0.9 and 32.2±1.0 Ma from its top (Meijer et al., 1983). Antiform and synform  
166 structures within the Alutom Formation are interpreted to be the result of volcano-tectonic collapse  
167 (Tracey et al., 1964), possibly related to paleotopography during deposition.

168         The Alutom Formation is overlain by the Oligocene to Miocene Umatac Formation, which is  
169 exposed in the south of Guam. The oldest, Oligocene, rocks of this formation are interbedded  
170 limestones, sandy and tuffaceous limestones, sandstones, and conglomerates (Siegrist and Reagan,  
171 2008). The Miocene lithologies of the Umatac Formation consist of basaltic andesitic pillow lavas,  
172 volcanic sandstones, breccias, and conglomerates, and medium to coarse-grained andesite flows  
173 (Siegrist and Reagan, 2008). The volcanic members of the Umatac Formation are highly weathered  
174 and only sporadically exposed. Bedding dips are mostly sub-horizontal, although some steeper dips  
175 up to 35° have been recorded in the west, where the Umatac Formation is in direct structural contact  
176 with the Facpi Formation (Siegrist and Reagan, 2008). As most of the Neogene formations have  
177 (sub)horizontal bedding planes, we interpret the steeper bedding dips in the west as related to  
178 paleotopography of the eroded pillow basalts on top of which the sediments were deposited and not  
179 as the result of deformation.



180

181 **Figure 2:** Simplified geological map of Guam (based on Siegrist and Reagan, 2008), showing the  
182 different sampling locations.

183

### 184 3. Sampling and analytical methods

185 Paleomagnetic samples with a standard diameter of 25 mm were collected with a water-cooled,  
186 petrol-powered drill. The orientation of the samples was measured using a magnetic compass with  
187 an inclinometer attached. We collected samples from six localities on the island of Guam from  
188 volcanic and sedimentary rocks. We collected a single core per basalt pillow or per sedimentary bed  
189 to optimize the chance of sampling individual spot readings of the paleomagnetic field with each  
190 core, following sampling procedures for paleomagnetic poles recommended by Gerritsen et al.  
191 (2022).

192 We collected samples from two localities in the Eocene Facpi Formation, from two localities  
193 in the Eocene-Oligocene Alutom Formation, and from two localities in the Miocene Umatac  
194 Formation (Figs 2 and 3). We collected samples from pillow basalts and lava flows at Facpi Point  
195 (FP1 and FP2; 63 samples) and Umatac Bay (UB; 34 samples). From the Eocene-Oligocene Alutom  
196 formation we collected samples from fine to coarse-grained turbiditic sandstones with volcanic  
197 detrital material and volcanic ash deposits at Mount Alutom (MA; 71 samples) and the Fonte River  
198 (AF; 64 samples). Collecting samples from Miocene rocks was complicated, as Miocene volcanic and  
199 volcanoclastic rocks exposed in Guam are highly weathered and only sporadically exposed, while  
200 Miocene limestones are often recrystallized. We collected 40 samples from coarse volcanoclastics of  
201 the Umatac Formation, at two relatively small road-sections along Highway 4 in the southernmost  
202 part of the island (KM1 and KM2 samples).

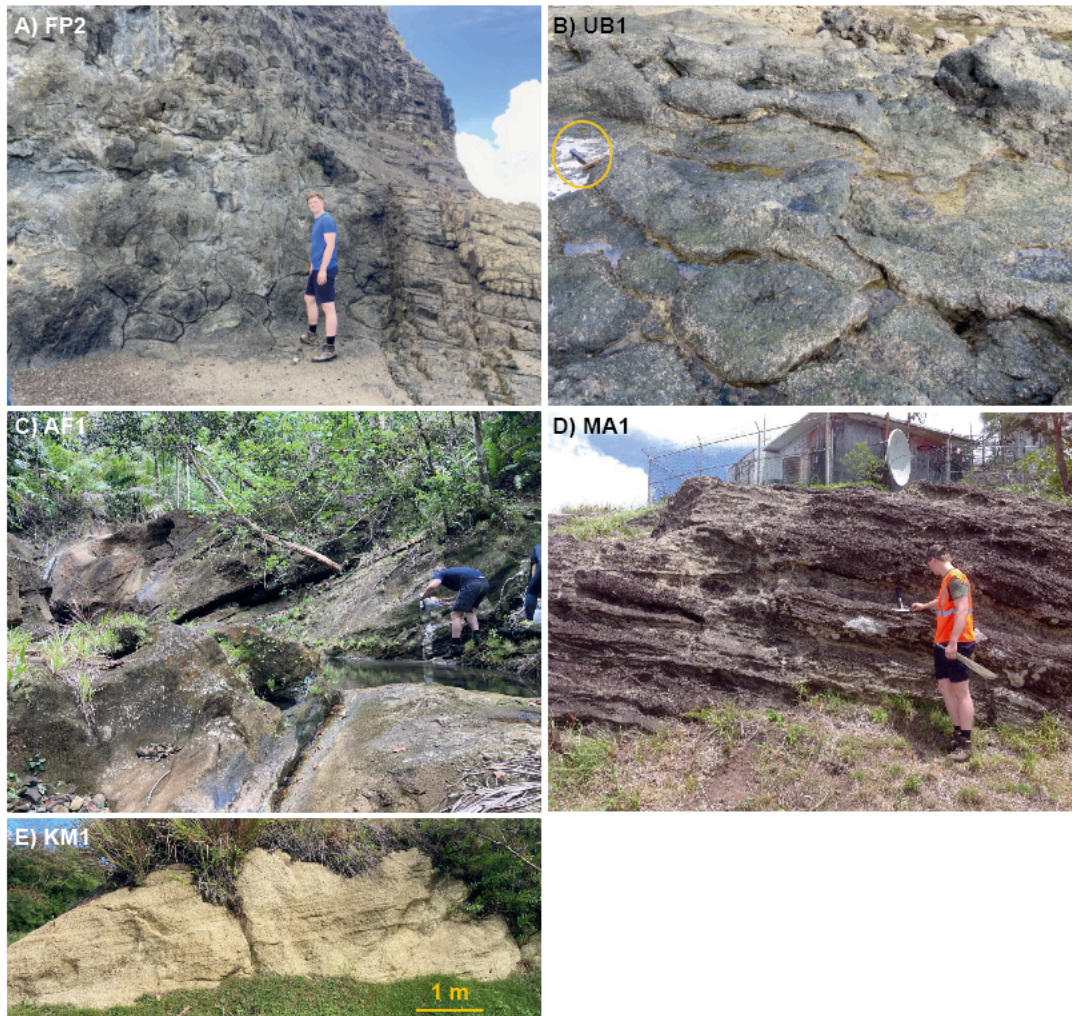
203 We carried out the paleomagnetic measurements at the paleomagnetic laboratory Fort  
204 Hoofddijk, Utrecht University (Utrecht, The Netherlands). Samples were either demagnetized using  
205 stepwise alternating field (AF) demagnetization in a robotized setup (Mullender et al., 2016) or  
206 stepwise thermal (TH) demagnetization. The magnetization was measured on a 2G DC-SQUID  
207 magnetometer. Throughout the demagnetization process, samples were kept in a magnetically  
208 shielded room.

209 Sample interpretation and statistical analysis was done using the online portal  
210 Paleomagnetism.org (Koymans et al., 2016, 2020). All our data are provided in the supplementary  
211 information and will be made available in the Paleomagnetism.org database (Koymans et al., 2020)  
212 as well as the MagIC database (Jarboe et al., 2012). Demagnetization diagrams were plotted as  
213 orthogonal vector diagrams (Zijderveld, 1967) and principal component analysis was used to the  
214 determine the characteristic remanent magnetizations (ChRM) component (Kirschvink, 1980). We  
215 used Fisher (1953) statistics on virtual geomagnetic poles following statistical procedures described  
216 in Deenen et al. (2011) to calculate site mean directions.

217 Thermomagnetic analyses were done with a modified horizontal translation Curie balance  
218 (Mullender et al., 1993) on selected samples from each locality to constrain the interpretation of the  
219 NRM components. The analysis was carried out in air and involved stepwise heating to 700 °C with  
220 intervened cooling to be able to discern potential thermochemical alteration due to the heating of the  
221 samples. The temperature sequence is as follows for most lithologies (in a cycling field between 200  
222 and 300 mT): room temperature 150 °C – 70 °C – 250 °C – 150 °C – 350 °C – 250 °C – 450 °C – 350 °C  
223 – 520 °C – 420 °C – 620 °C – 500 °C – 700 °C – room temperature. Where deemed appropriate the  
224 150 °C segment with corresponding cooling to 70 °C was omitted. Curie temperatures are  
225 determined with the two-tangent method (Grommé et al., 1969). Each ChRM is interpreted with a  
226 minimum of four consecutive demagnetization steps. AF demagnetization steps affected by  
227 gyroremanent magnetization (Dankers and Zijderveld, 1981) were not used for ChRM interpretation.  
228 Where two components unblocked simultaneously and decay did not trend towards the origin, we  
229 used great circle interpretation (McFadden and McElhinny, 1988). In general, we interpreted ChRM



230 directions without forcing the component through the origin, unless demagnetization behavior was  
231 noisy. We did not apply a maximum angular deviation cut-off, because Gerritsen et al. (2022) showed  
232 that this makes no difference for the precision or position of the final paleomagnetic pole, but we  
233 note that the widely-used MAD-cutoff of 15° would not have eliminated data. Finally, we applied a  
234 45° cutoff to eliminate outliers, but this omitted <5% of the data.  
235



236  
237 **Figure 3:** Field photos of the different sampling locations. A and B) Pillow basalts and cross-cutting  
238 dike of the Eocene Facpi Formation; C and D) Volcaniclastics of the Oligocene Alutom Formation. E)  
239 Coarse pyroclastics from the Miocene Umatac Formation.

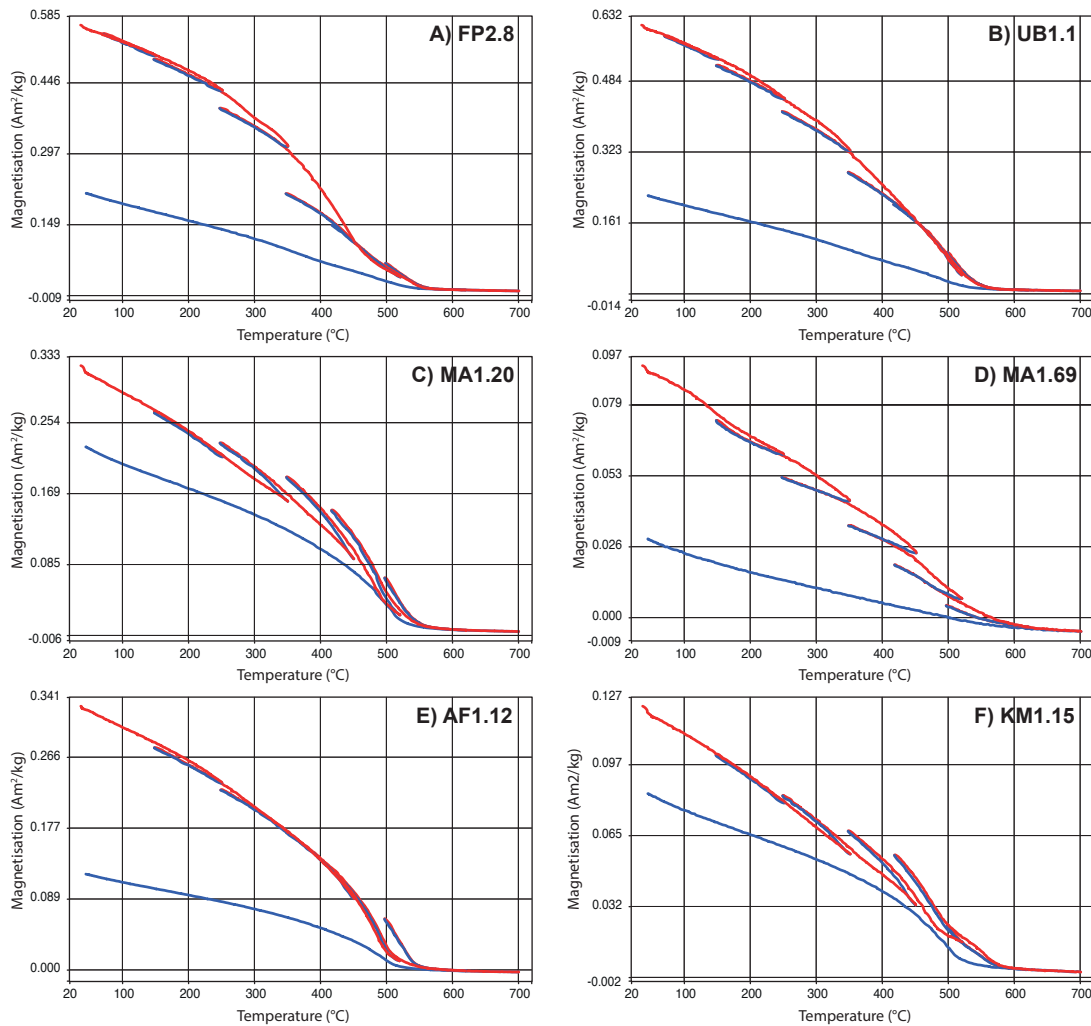
240

## 241 4. Results and Interpretation

### 242 4.1. Thermomagnetic results

243 The Eocene Facpi Formation pillow lavas (FP2.8 and UB1.1, ~0.5-0.6 Am<sup>2</sup>/kg) are strongly magnetic,  
244 as expected for basaltic lavas (Fig. 4a-b). On heating in air, they oxidize to a variable extent. Barely or  
245 no oxy-exsolution is observed; it would be manifested by a corresponding cooling segment above the  
246 previous heating segment pointing towards formation of iron-richer titanomagnetite. FP2.8 shows  
247 two Curie temperatures, at ~470 °C and ~560 °C indicating titanomagnetite with a variable amount

248 of Ti substitution. On heating to 700 °C, oxidation to less magnetic material, presumably hematite, is  
 249 noted because the final cooling curve is below the heating segments. UB1.1 only shows the higher  
 250 Curie temperature, at ~560-570 °C indicating a very low level of Ti substitution. The Oligocene rocks  
 251 of the Alutom Formation (~0.1 to 0.3 Am<sup>2</sup>/kg; MA1.20, MA1.69; AF1.12; Fig. 4c-e) are less magnetic  
 252 than the Eocene rocks. AF1.12 is essentially reversible up to 520 °C with only minute oxidation. Curie  
 253 temperature is estimated at ~500-520 °C. Some oxy-exsolution appears in the next heating segment  
 254 (and rises the Curie temperature). On further heating to 700 °C oxidation to less magnetic material is  
 255 noted (Curie temperature remains at 500-520 °C). MA1.20 shows prominent oxy-exsolution across a  
 256 large temperature interval: already after heating to 350 °C the behavior is visible which makes  
 257 determination of the original Curie temperature tedious. MA1.69 is the weakest Oligocene sample; it  
 258 behaves like FP2.8. The Miocene sample (KM1.15) is not that magnetic (~0.1 Am<sup>2</sup>/kg) and shows  
 259 prominent oxy-exsolution from 350 °C upward (Fig. 4). Oxidation at the highest temperature leads to  
 260 a final cooling curve below the heating curves.  
 261



262

263 **Figure 4:** Results of thermomagnetic analysis. Heating segments are in red, cooling segments are in

264 blue.

265

## 266 **4.2. Paleomagnetic results**

### 267 **4.2.1. Facpi Formation**

268 Paleomagnetic samples from the different sampling locations in the Facpi Formation basalts  
269 provided uniform demagnetization behavior. Thermal as well as AF demagnetization yielded small  
270 viscous overprints that were generally cleaned by 150°C, occasionally up to 270°C, or 10-15 mT, after  
271 which specimens decayed to the origin. Thermally demagnetized samples lost their signal after  
272 heating until ~510-580°C, consistent with (titano-)magnetite as carrier, whereas AF  
273 demagnetization often started to deviate from the path towards the origin at fields of ~50 mT and  
274 higher. We interpret the latter behavior as gyroremanent magnetization (Dankers and Zijdeveld,  
275 1981), which is common for (titano-)magnetite-bearing basalts (e.g., van Hinsbergen et al., 2010).  
276 We interpreted the component decaying towards the origin as the ChRM, typically unblocking  
277 between ~180 and 580°C, or between 15 and 50 mT (as at higher levels gyroremanent  
278 magnetization may interfere).

279 Thermal and AF demagnetization yielded similar directions (Fig. 5a, b). We corrected our  
280 paleomagnetic results for bedding strikes and dips of 349/20° E and 356/20° E in the FP and UB  
281 sites, respectively. We report both geographic (in-situ) and tectonic (tilt-corrected) results in Table 1,  
282 but limit our analysis to the tilt-corrected results, as these are interpreted as being representative of  
283 the paleomagnetic signal at the time of formation of the rock. The majority of samples yielded  
284 magnetic directions with shallow inclinations, and with northeasterly declinations (Fig. 5c, d). A  
285 small cluster of 7 stratigraphically consecutive samples in the UB locality has opposite polarity (Fig.  
286 5a, b; Fig. 6b). We exclude outliers by applying a 45° cut-off, which eliminates a few directions. The  
287 opposite polarities (N=28 vs N=7) yield antipodal declinations, but the smaller dataset has a steeper  
288 inclination than the larger dataset (in geographic coordinates; Fig. 6b) such that a reversals test (of  
289 Tauxe et al, 2010) as implemented in Paleomagnetism.org (Koymans et al., 2016) is negative. We  
290 interpret this as the result of insufficient averaging of paleosecular variation (PSV) in the small  
291 dataset and consider the presence of reversals in the sequence as a signal that the ChRM is primary.  
292 The FP sampling locations were cut by dikes with thicknesses up to ~5 m. To evaluate whether the  
293 intrusion of these dikes may have remagnetized the surrounding pillow lavas, we collected 5-8  
294 samples each from one dike cutting FP1 and three dikes cutting FP2. These dikes yielded K-values of  
295 17-130. The K-values (between 17 and 57) of three of the dikes are consistent with PSV-induced  
296 scatter (Deenen et al., 2011), suggesting that they cooled gradually, and each sample represents a  
297 spot reading of the field, while the K-value (130) of the fourth dike suggests rapid cooling, which  
298 means that this dike represents a single spot-reading. In addition, while the average directions of the  
299 dikes and the lavas are northeasterly, they are not identical to the clusters from the pillow lavas (Fig.  
300 6a). The scatter within and difference between the average directions of the dikes and the pillow  
301 lavas is straightforwardly explained by the low number of samples underpinning these averages (see  
302 Vaes et al., 2022). These results therefore do not suggest that dike intrusion remagnetized the

303 surrounding pillow lavas, but rather that the samples collected from the pillow lavas and dikes each  
304 may be considered a spot reading from the paleomagnetic field.

305 We computed a grand average for the FP locations and for the UB location (Fig. 6c; Table 1),  
306 which are located 6 km apart. The FP locations yielded a direction of Dec/Inc =  $37.3 \pm 4.5^\circ / -8.2 \pm 8.8^\circ$   
307 (N=72, K=15.0, A95=4.5) and the UB location yielded a direction of Dec/Inc =  $71.9 \pm 4.6^\circ / -15.0 \pm 8.7^\circ$   
308 (N=35, K=29.1, A95=4.6). Both pass the Deenen et al. (2011) criteria, suggesting that their data  
309 scatter can be straightforwardly explained by PSV alone. The inclinations of both localities are very  
310 similar (paleolatitudes of  $4.1^\circ$  and  $7.6^\circ$  N or S; Fig 6c), but the declinations reveal a  $\sim 35^\circ$  difference  
311 in vertical axis rotation. A southern hemisphere normal component would require clockwise  
312 rotations of  $37^\circ$  and  $72^\circ$  relative to the present-day GAD field, a northern hemisphere reversed  
313 component would require counterclockwise rotations of  $147^\circ$  and  $108^\circ$ , respectively. We consider the  
314 smaller rotations the most likely and use these in the data compilation.

315

#### 316 **4.2.2. Alutom and Umatac Formations**

317 Demagnetization diagrams of the MA section display varying demagnetization behavior throughout  
318 the section that is characterized by consecutive samples with similar behavior that strongly differs  
319 from subsequent parts of the section. This is probably owing to the volcanoclastic nature of the  
320 section, whereby beds may represent volcanic events, as well as intra-volcanic sedimentary deposits.  
321 First, the magnetization intensity varies strongly, from several 10.000 to several million  $\mu\text{A}/\text{m}$ .  
322 Second, the magnetizations, typically showing decay towards the origin, display varying degrees of  
323 overprinting. South-directed (likely reverse) overprints occur on north-directed magnetizations and  
324 vice versa (Fig. 5e, 5f). These may represent recent overprints of a normal field over a primary  
325 reverse magnetization, but also an overprint induced by a volcanic episode during a reverse polarity  
326 state of the field over a primary normal magnetization. In addition, the presence of volcanic events is  
327 suggested by the tight clustering of directions of consecutive samples in the section. For example,  
328 samples MA1.50-MA1.56 show a tightly clustered reverse magnetization ( $k=250$ ,  $n=7$ ), an overlying  
329 sequence of MA1.58-1.66 yield a nearly antipodal direction with a  $k$ -value of 133 ( $n=8$ ) (Fig. 6d).  
330 Such tight clustering is much higher than may be expected from PSV (Deenen et al., 2011) and likely  
331 represent paleomagnetic spot readings recorded in discrete volcanic events.

332 When all dominant magnetizations, i.e., of the components that decay towards the origin, are  
333 combined into a single plot, it is evident that clusters of opposite polarity are present in the section,  
334 as well as a large cluster of data around the recent paleomagnetic field direction. We suspect that the  
335 magnetizations include recently remagnetized and primary magnetizations (Fig. 6d). Because we  
336 cannot establish with certainty per sample which directions are overprints and which are primary,  
337 and because of the evidence that sets of primary directions may represent single spot readings of the  
338 field, we do not consider the directions we determined as a reliable indicator of the paleomagnetic  
339 field. We refrain from using the paleomagnetic data from MA for further analysis. Samples of section

340 AF typically display gradual decay towards the origin defining single components with little  
341 overprint. In some cases, the magnetization is only carried by carriers that lost their magnetization  
342 by  $\sim 20$  mT, after which only erratic behavior remains (Fig. 5g). We interpret these samples as only  
343 carrying a recent overprint. The remainder of samples demagnetized typically until 50-60 mT or  
344  $\sim 270$  and  $500^\circ\text{C}$ , after which only erratic behavior of low-intensity magnetization remained (Fig. 5h,  
345 5i). Interpreting the components that decay towards the origin as the ChRM leads to a tight cluster of  
346 directions with  $D = 352.2 \pm 2.0$ ;  $I = 23.0 \pm 3.5$ ;  $K = 47.5$ ,  $A95 = 2.0$ ,  $N=113$ . The clustering of the data is  
347 tight (Fig. 6e) but may still be explained by PSV ( $A95_{\min}$  *sensu* Deenen et al. (2011) for  $N=113$  is 1.8).  
348 Because the bedding is changing orientation throughout the section, varying in dip by  $\sim 25^\circ$ , we  
349 performed a fold test, which is clearly negative (Fig. 6g). The paleolatitude computed from the  
350 paleomagnetic direction in geographic coordinates is  $\sim 12^\circ$ , which corresponds to the latitude of the  
351 sampling location. This, combined with the solely normal magnetization leads us to interpret the  
352 magnetization of section AF as a recent overprint, whereby the small counterclockwise rotation may  
353 reflect the effects of e.g., land sliding or otherwise minor, recent deformation.

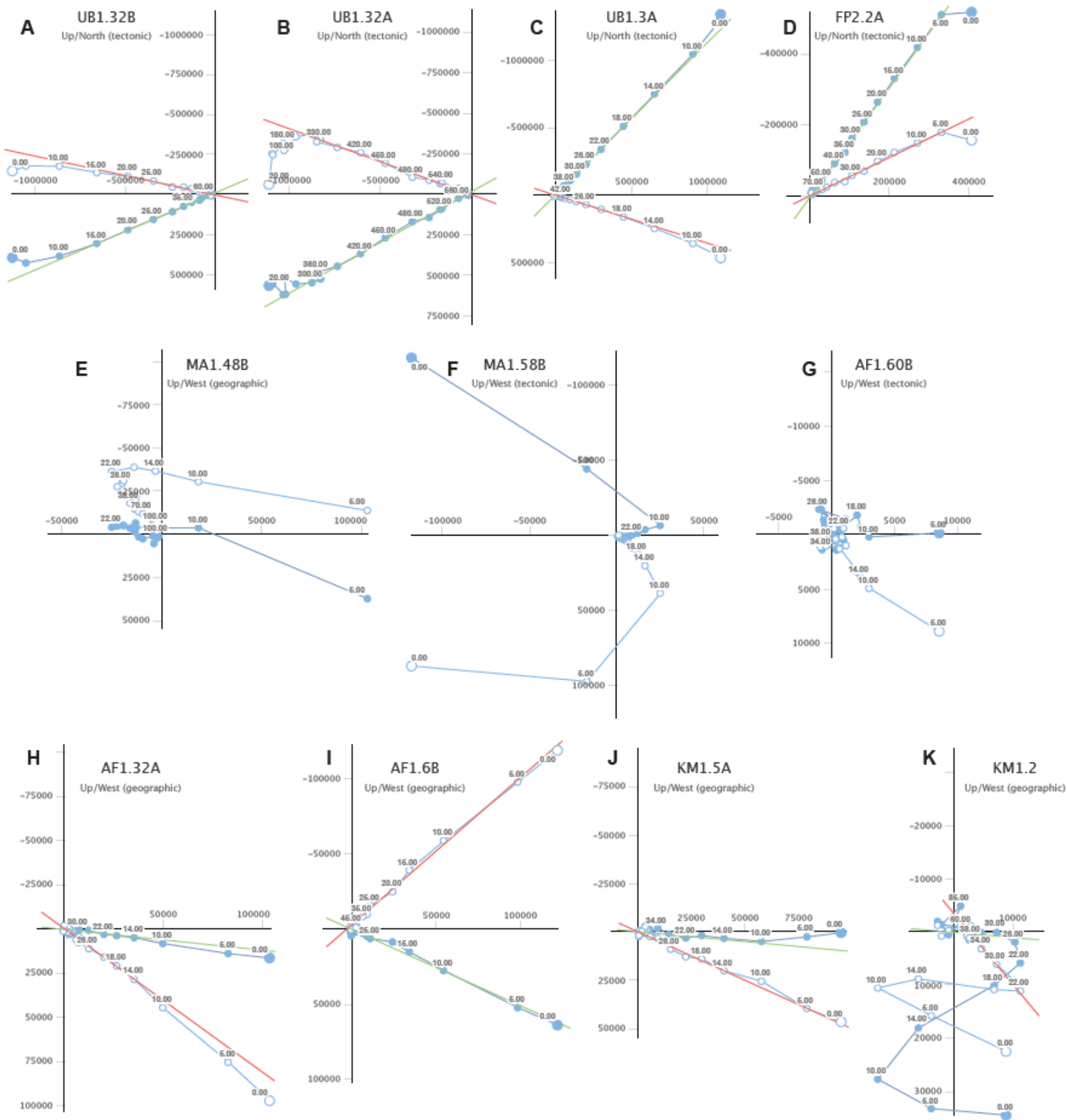
354 Finally, the Miocene sites of KM display demagnetization behavior that is similar to that of  
355 site AF. A minor viscous overprint is typically demagnetized by 10 mT (Fig. 5j), although non-  
356 systematic overprint directions are occasionally demagnetized until  $\sim 20$  mT (Fig. 5k), after which  
357 demagnetization decays to the origin until  $\sim 50$  mT. At higher demagnetization steps, decay becomes  
358 noisy. Thermal demagnetization diagrams are incomplete because the loose samples disintegrated  
359 during thermal demagnetization. Interpreting the magnetizations that decay towards the origin as  
360 the ChRM leads to a clustering of normal polarity, north-directed directions. The average direction is  
361  $D = 355.7 \pm 6.4^\circ$ ,  $I = 21.4 \pm 11.4^\circ$ ,  $K=15.3$ ,  $A95 = 6.3$ ,  $N=36$  (Fig. 6f; Table 1). This is an insignificant  
362 difference with the recent GAD direction predicted for the sampling location. A fold test is permitted  
363 because there is bedding orientation variation. This fold test gives optimal clustering at  $<0\%$   
364 unfolding, which may suggest that some folding of an originally undulating sedimentary cover  
365 occurred prior to magnetization. The cluster of paleomagnetic directions may in principle be  
366 explained by PSV ( $A95_{\min, \max} = 2.9, 8.6$  *sensu* Deenen et al., 2011). Nonetheless, the insignificant  
367 difference between the average direction in geographic coordinates with the recent field, combined  
368 with the negative fold test leads us to not consider this result as a primary magnetization from which  
369 we may infer tectonic motion of Guam since the Miocene. Combined, we do not interpret the samples  
370 from the two Oligocene sections or the Miocene sites to carry a resolvable primary magnetization,  
371 and where it may, it does not represent a long-term GAD direction with representative PSV scatter.

372 **Table 1:** Paleomagnetic results

<b>Geographic (in situ) coordinates</b>															
Locality	Latitude (°N)	Longitude (°E)	N	Ns	Dec (°)	Inc (°)	k	a95	K	A95	A95Min	A95Max	$\Delta D_x$ (°)	$\Delta I_x$ (°)	$\lambda$ (°)
FP	13.3419843	144.636729	73	79	37.05	7.65	9.15	5.81	14.72	4.48	2.16	5.49	4.49	8.83	3.84
UB	13.29565	144.6597	36	38	73.52	3.94	15.9	6.18	23.7	5.01	2.86	8.58	5.01	9.99	1.97
AF	13.459	144.73102	113	121	352.17	23.04	35.49	2.26	47.52	1.95	1.81	4.17	1.99	3.45	12.01
MA	13.43244	144.7129	69	79	9.98	18.08	13.9	4.75	18.52	4.08	2.21	5.69	4.13	7.57	9.27
KM	13.249215	144.716595	36	46	355.67	21.36	9.4	8.24	15.3	6.31	2.86	8.58	6.43	11.37	11.06
<b>Tectonic (tilt-corrected) coordinates</b>															
Locality	Latitude (°N)	Longitude (°E)	N	Ns	Dec (°)	Inc (°)	k	a95	K	A95	A95Min	A95Max	$\Delta D_x$ (°)	$\Delta I_x$ (°)	$\lambda$ (°)
FP	13.3419843	144.636729	72	79	37.26	-8.19	9.47	5.74	14.98	4.47	2.17	5.54	4.48	8.8	-4.12
UB	13.29565	144.6597	35	38	71.92	-14.96	18.14	5.85	29.14	4.57	2.89	8.73	4.61	8.68	-7.61
AF	13.459	144.73102	113	121	335.05	40.45	23.14	2.82	24.13	2.76	1.81	4.17	3	3.78	23.09
MA	13.43244	144.7129	71	79	4.45	8.5	13.79	4.7	22.55	3.62	2.18	5.59	3.63	7.13	4.28
KM	13.249215	144.716595	33	46	346.1	21.77	8.65	9.03	14.11	6.9	2.96	9.06	7.04	12.38	11.29

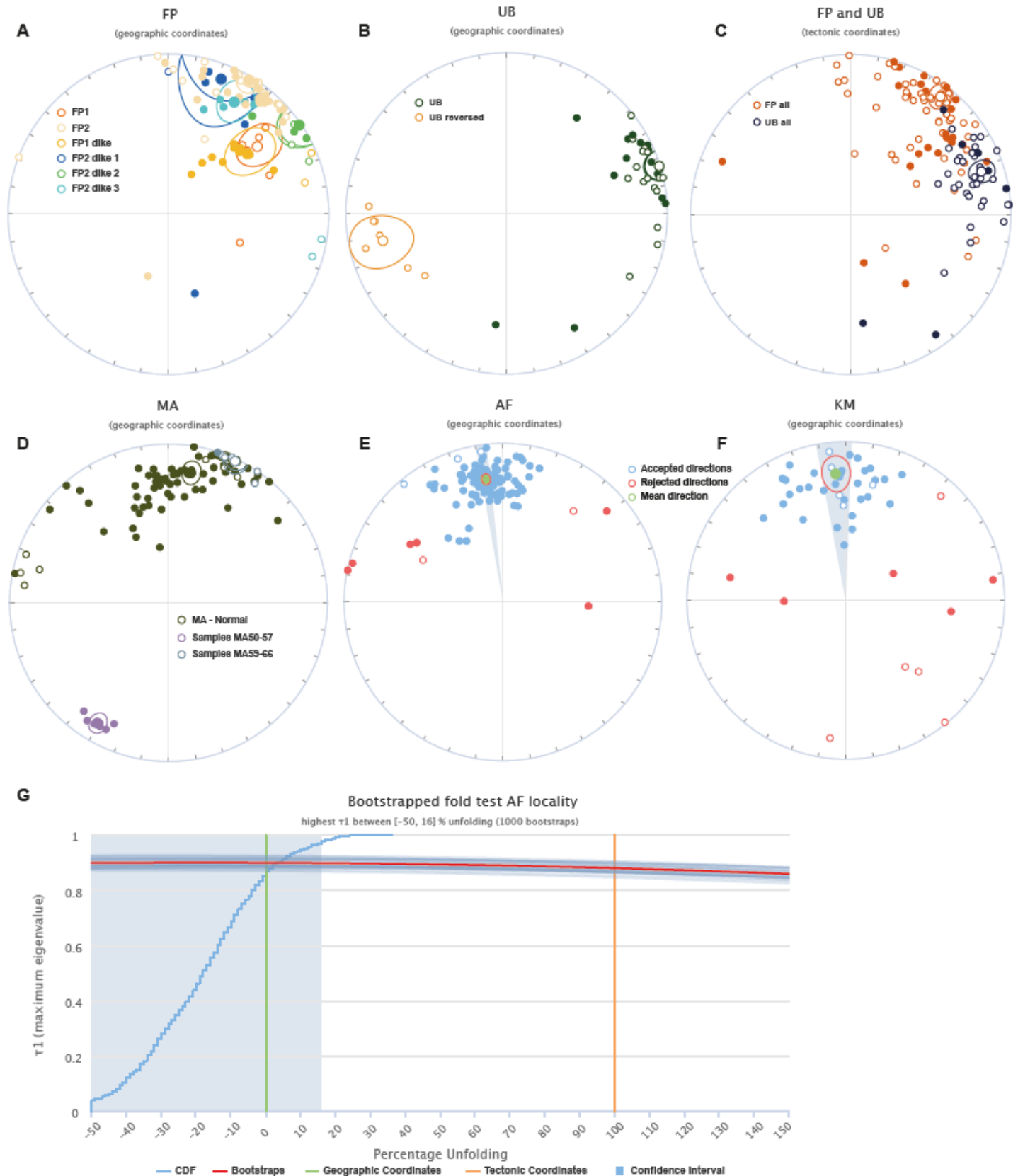
373 N: number of samples; Ns: Number of samples that are used for the analysis after 45° cut-off; Dec: Declination; Inc: Inclination;  $\Delta D_x/\Delta I_x$ : uncertainty in  
 374 declination/inclination;  $\lambda$ : paleolatitude

375



376 **Figure 5:** Zijdeveld demagnetization diagrams of selected samples. Closed circles for declination, open

377 circles for inclination. Numbers along axes are intensities in  $\mu\text{A/m}$



378

379 **Figure 6:** Paleomagnetic results from the different sections. A-F) Paleomagnetic directions and means  
 380 of the different sampled sections. Open (closed) symbols are up (down) directions. G) Fold test of the AF  
 381 locality.



## 382        **5. Paleomagnetic data compilation**

383 We compiled published paleomagnetic data from the PSP, to which we added our two sites from the  
384 Eocene Facpi Formation of Guam that were interpreted as primary directions. The database contains  
385 data from boreholes that drilled into igneous basement, and from field localities in the Philippines  
386 and the northern Maluku islands, from Palau, Guam, the Northern Mariana, and Ogasawara islands.  
387 We compiled site-level data as originally published, whereby we followed the authors'  
388 interpretations about magnetic field polarity and whether bedding tilt corrections were applicable.  
389 We subsequently calculated mean paleomagnetic directions from collections of similar age and  
390 locations, using the online portal Paleomagnetism.org (Koymans et al., 2016, 2020), whereby we  
391 assumed that each reported direction, i.e., a lava site, represents a spot reading of the magnetic field,  
392 regardless of its k-value. If an antipodal paleomagnetic direction is present within a locality, we  
393 flipped the polarity and combined the data into one collection before calculating the locality mean.  
394 Before calculation of the paleomagnetic mean direction, we excluded sites if they were rejected by  
395 the original authors. In addition, we did not calculate means for localities with fewer than 4 sites  
396 (spot readings). Our calculated means may differ from the originally published mean direction, for  
397 example when the authors mixed sedimentary sites with igneous sites, which we kept separate. We  
398 applied a 45° cut-off to exclude outliers and transitional directions before recalculation of mean  
399 directions. After recalculation of mean paleomagnetic directions, we excluded localities with K values  
400 (Fisher (1953) precision parameters on poles) below 10 (following Meert et al., 2020) or when  
401 means yielded an A95 outside the A95min-max confidence envelope of Deenen et al. (2011). Our  
402 recalculated means are provided in Table 2, while the site-level compilation is provided in  
403 Supplementary Table S1. A total of 20 paleomagnetic poles in our PSP compilation passed our quality  
404 criteria, obtained from lava flows, pillows, or dikes, as well as 7 paleolatitudes obtained from  
405 boreholes.

406        Paleomagnetic data obtained from sedimentary rocks were not added to the compilation,  
407 because it is unclear whether the reported sites represent spot-readings of the field or whether a  
408 site adequately averages PSV. In addition, the number of samples collected at the sedimentary  
409 localities is insufficient (i.e., <80-100, see Tauxe and Kent, 2004; Vaes et al., 2021) to properly apply  
410 the E/I inclination shallowing correction (Tauxe and Kent, 2004), prohibiting using these data to  
411 assess paleolatitudinal motion. In a few cases, paleomagnetic datasets obtained from sedimentary  
412 rocks of boreholes contain sufficient samples to correct for inclination shallowing, especially large  
413 magnetostratigraphic sections, but individual directional data is needed for the E/I correction. Also,  
414 these borehole data do not contain declination data because they are not azimuthally oriented.  
415 Recently, declination data from a borehole in the PSP were obtained from an oriented core (Yamazaki  
416 et al., 2021). However, the uncertainty on these data remains unknown and with their limited  
417 number of samples (13 samples from each of two cores of c. 30 cm), the data cannot be used for  
418 paleolatitude constraints. For these reasons, all sedimentary data are excluded from our compilation.

119 **Table 2:** Paleomagnetic data compilation (field sites only)

Location	Age (Ma)	Lat (°N)	Lon (°E)	N	Ns	Dec (°)	Inc (°)	k	a95	K	A95	A95Min	A95Max	$\Delta D_x$ (°)	$\Delta I_x$ (°)	$\lambda$ (°)	Reference
C. Cordillera	2.6±2.6	16.672	120.822	6	6	349.88	30.59	23.71	14.04	20.87	15.01	5.86	26.52	15.67	24.19	16.46	Queaño et al. (2007)
Batangas	7.0±0.8	13.7	121.2	6	6	318.28	35.35	39.34	10.81	38.76	10.9	5.86	26.52	11.57	16.32	19.53	Fuller et al. (1991)
C. Cordillera	10.2±4.9	18.062	120.998	7	8	274.88	20.65	23.71	12.65	29.32	11.33	5.51	24.07	11.54	20.55	10.67	Queaño et al. (2007)
Obi*	11±1	-1.58	127.83	4	4	14.17	-41.89	452.72	4.32	368.69	4.79	6.89	34.24	5.25	6.38	-24.15	Ali and Hall (1995)
Obi	11.3±3.0	-1.52	127.95	9	9	327.78	-25.91	57.2	6.87	103.87	5.08	4.98	20.54	5.22	8.7	-13.65	Ali and Hall (1995)
Saipan	12±3	15.13	145.71	5	5	28.76	31.87	57.07	10.21	79.36	8.64	6.3	29.75	9.05	13.67	17.27	Haston and Fuller (1991)
C. Cordillera	14.2±8.9	16.45	120.8	4	4	315.49	7.73	39.8	14.74	50.46	13.06	6.89	34.24	13.09	25.76	3.88	Fuller et al. (1991)
Sierra Madre	16.04±4.41	15.368	121.24	5	5	297.55	19.14	17.96	18.55	18.31	18.37	6.3	29.75	18.65	33.77	9.85	Queaño et al. (2007)
Palau	20.1±0.5	7.37	134.52	5	5	54.48	3.48	20.31	17.39	32.69	13.58	6.3	29.75	13.59	27.09	1.74	Haston et al. (1988)
Guam	28.5±5.5	13.45	144.7	4	4	57.67	10.73	61.13	11.85	98.58	9.3	6.89	34.24	9.34	18.12	5.41	Haston and Fuller (1991)
Kasiruta	32.3±3.0	1.18	128.31	9	9	40.49	-24.68	27.64	9.97	29.61	9.62	4.98	20.54	9.87	16.72	-12.94	Hall et al. (1995)
Saipan	35.8±1.9	15.23	145.8	11	12	42.09	-8.68	13.2	13.05	21.31	10.12	4.6	18.1	10.15	19.9	-4.37	Haston and Fuller (1991)
Guam	43.8±2.6	13.296	144.660	35	38	71.92	-14.96	18.14	5.85	29.14	4.57	2.89	8.73	4.61	8.68	-7.61	This study
Guam	43.8±2.6	13.342	144.637	72	79	37.26	-8.19	9.47	5.74	14.98	4.47	2.17	5.54	4.48	8.8	-4.12	This study
Hahajima	45±7	27.08	142.16	7	7	32.69	2.86	11.24	18.82	19.43	14.04	5.51	24.07	14.05	28.03	1.43	Kodama et al. (1983)
Sierra Madre	45±11	17.216	122.313	7	7	230.18	-2.7	19.93	13.86	30.41	11.12	5.51	24.07	11.13	22.21	-1.35	Queaño et al. (2007)
Anijima	45±7	27.12	142.21	14	16	86.84	9.04	7.41	15.66	14.22	10.92	4.18	15.55	10.96	21.44	4.55	Keating et al. (1983)
Chichijima	45±7	27.08	142.21	25	27	104.96	9.98	6.77	12.04	10.54	9.37	3.31	10.79	9.4	18.31	5.03	Kodama et al. (1983)
Zambales	46.4±5.3	15.657	120.057	6	6	288.7	-0.1	17.64	16.4	49.39	9.63	5.86	26.52	9.63	19.25	-0.05	Fuller et al. (1989)
Zambales	46.4±5.3	15.56	120.08	13	13	235.29	-1.96	18.85	9.8	36.67	6.94	4.3	16.29	6.94	13.86	-0.98	Fuller et al. (1989)
C. Cordillera*	67±33	17.17	121.06	5	5	159.26	-12.47	162.46	6.02	400.54	3.83	6.3	29.75	3.85	7.39	-6.31	Queaño et al. (2009)
Samar	99.0±3.9	11.1	125.25	13	13	341.6	-26.6	14.69	11.19	25.88	8.3	4.3	16.29	8.56	14.11	-14.06	Balmater et al. (2015)

120 \*A95 outside of Deenen et al. (2011) confidence ellipse

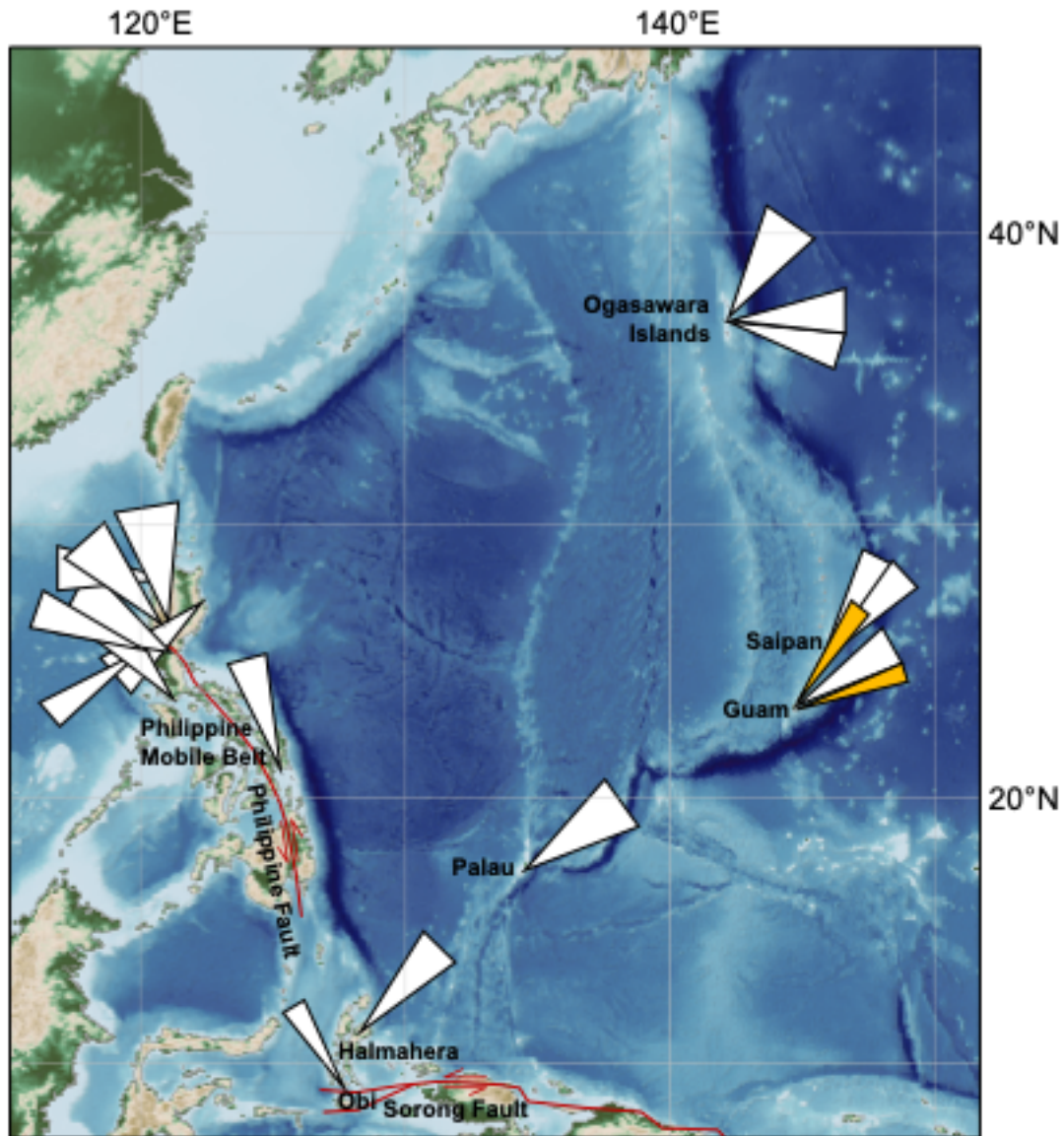
121 N: number of samples; Ns: Number of samples that are used for the analysis after 45° cut-off; Dec: Declination; Inc: Inclination;  $\Delta D_x/\Delta I_x$ : uncertainty in declination/inclination;  $\lambda$ :  
122 paleolatitude

423        **6. Discussion**

424        Determining the vertical axis rotation of the PSP using paleomagnetic data is not straightforward.  
425        First, datasets are typically small ( $N < 10$ ) and the dispersion of such datasets around the true pole is  
426        often larger than suggested by their A95 error margins, and the reliability varies with  $N$  (Vaes et al.,  
427        2022). Both easterly and westerly declinations have been obtained, generally westerly in the  
428        northern Philippines, and generally easterly on the islands in the south and east of the plate (Fig. 7).  
429        However, which of these declinations, if any, are representative for the rotation history of the plate as  
430        a whole is difficult to assess given that all locations come from its deformed plate margins. The  
431        Philippine Mobile Belt, which comprises PSP's western boundary, is cross-cut by major left-lateral  
432        strike slip faults, including the 1200 km long Philippine Fault (Aurelio et al., 1991), which are bound  
433        to induce local block rotations (Queaño et al., 2007, 2009). Similarly, the northern Maluku islands,  
434        including Halmahera and Obi, are in the south crosscut by the Sorong Fault system and are in an  
435        upper plate position relative to the Halmahera trench (Fig. 7). This position in a tectonically active  
436        region increases the likelihood of local block rotations, as shown by the strongly varying  
437        paleomagnetic declinations (Ali and Hall, 1995; Hall et al., 1995a). Moreover, a problem with  
438        paleomagnetic data from igneous rocks, often from stratovolcanoes of arcs, is that structural control  
439        on bedding tilt is generally poor, and the effect of small tectonic tilts on large primary bedding dips  
440        cannot be seen in the field.

441        Whether local deformation played a role in the paleomagnetic data obtained from the islands  
442        along the eastern margin of the PSP was less well-defined. The declination difference of  $35^\circ$  that we  
443        obtained from two Eocene localities in Guam shows that local block rotations also played a role in  
444        the forearc of the Mariana Trench. All paleomagnetic poles from the eastern PSP margin that pass  
445        our quality criteria have been interpreted as an easterly deflection of the magnetic field (Fig. 7).  
446        However, due to their sub-equatorial paleolatitude, the polarity of these data, and hence the sense of  
447        rotation, is not well known (Kodama et al., 1983; Haston and Fuller, 1991). Moreover, most reliable  
448        paleomagnetic poles obtained from the eastern margin of the plate were obtained from the southern  
449        forearc regions, i.e., Saipan, Guam, and Palau. The curved shape of the Mariana and Palau arcs makes  
450        interpreting these data as unequivocal evidence of plate-wide rotations difficult to defend.

451



452  
453 **Figure 7:** Map of the Philippine Sea Plate showing declinations in our paleomagnetic data compilation  
454 with A95 confidence parachutes. White parachutes mark previously published paleomagnetic data,  
455 yellow parachutes mark our new paleomagnetic data from Guam. Base map is ETOPO 2022 15 Arc-  
456 Second Global Relief Model (NOAA National Centers for Environmental Information, 2022).

457  
458 Despite the limited number and the questionable use of paleomagnetic data to infer whole-  
459 PSP motion, many plate motion models suggest that the Philippine Sea Plate underwent a large-scale  
460 clockwise rotation, of about 90° (e.g., Hall et al., 1995a; Yamazaki et al., 2010; Seton et al., 2012; Wu  
461 et al., 2016; Liu et al., 2023). This idea was originally proposed based on the first paleomagnetic  
462 results from the Philippine Sea Plate (Keating and Helsey, 1985; Haston et al., 1988; Haston et al.,  
463 1991), although some authors suspected that local vertical-axis rotations resulting from arc bending  
464 or forearc rotation were actually more realistic (McCabe and Uyeda, 1983; Keating et al., 1983;

465 Kodama et al., 1983; Seno and Maruyama, 1984). Subsequently, based on data from the northern  
466 Maluku islands, Hall et al. (1995a) suggested that the PSP underwent a 50° clockwise rotation  
467 between 50 and 40 Ma, no rotation between 40 and 25 Ma, and an additional 35° clockwise rotation  
468 between 25 and 5 Ma. More recent studies compiled paleomagnetic data (e.g., Wu et al., 2016), and  
469 some studies questioned the validity of some of the existing paleomagnetic data, including the  
470 possibility of local block rotations and raised the issue whether some localities, such as Halmahera,  
471 have been part of the PSP throughout the Cenozoic (Xu et al., 2014; Zahirovic et al., 2014; Wu et al.,  
472 2016). However, the quality of the existing data was never assessed in detail using recent quality  
473 criteria (Meert et al., 2020; Vaes et al., 2021; Gerritsen et al., 2022) and it was thus never quantitatively  
474 assessed whether the existing paleomagnetic data are reliable to infer PSP motions. Therefore,  
475 despite the suspicion of compromised data, the idea of a large-scale clockwise rotation of the entire  
476 PSP plate is still widely used, and recent plate tectonic reconstructions often assumed c. 90°  
477 clockwise rotation, citing paleomagnetic data (Seton et al., 2012; Wu et al., 2016; Liu et al., 2023).

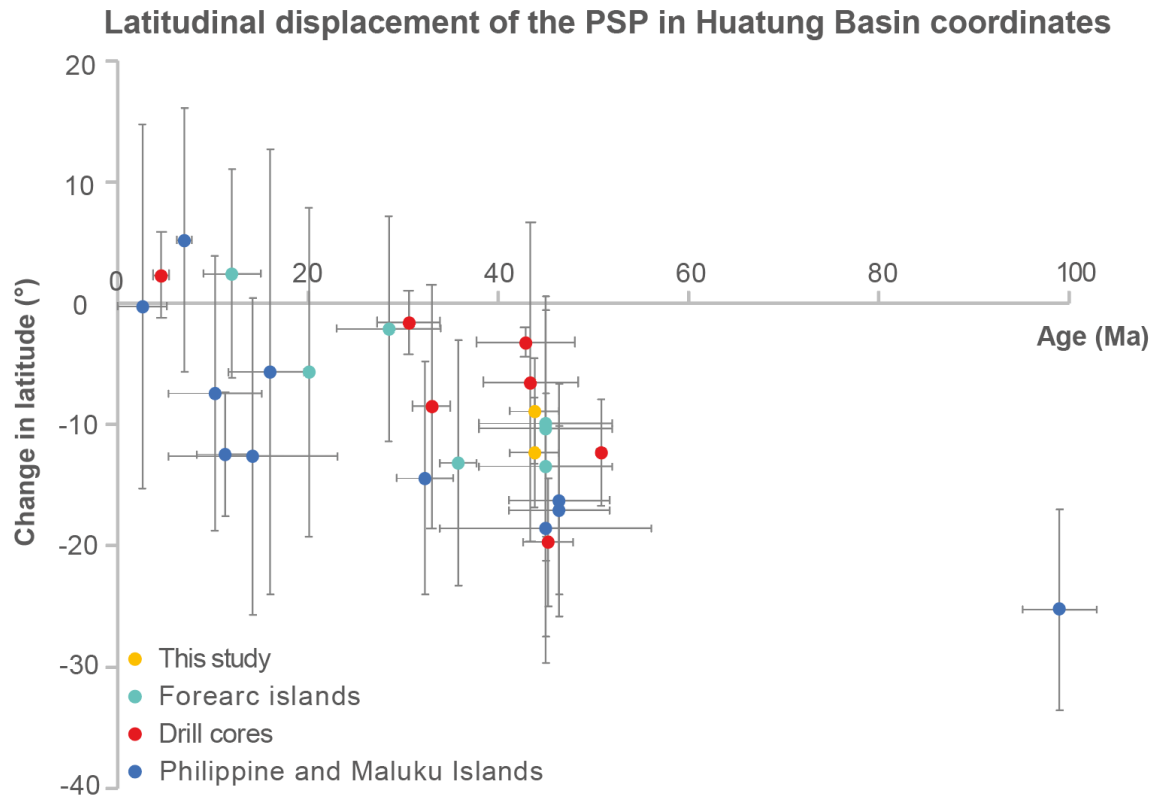
478         Based on our new compilation of PSP paleomagnetic data, however, we find that the  
479 paleomagnetic data base is not of sufficient quality to form a basis to invoke rotation of the entire  
480 plate. Notably, the quality criteria that we used for the compilation in this paper are loose compared  
481 to those of Meert et al. (2020). If we were to apply the criterion of Meert et al. (2020) that each  
482 locality should include at least 8 sites (spot-readings), only nine paleomagnetic results would pass, of  
483 which two are from this study, and our data reveal strong local rotations. Applying additional criteria  
484 of Meert et al. (2020), one of the nine remaining poles would be discarded because of its K-value >70,  
485 even though it passes the Deenen et al. (2011) criteria, and our two new poles would be discarded  
486 because we did not take a minimum of 3 samples per individual lava flow (even though doing so  
487 cannot be demonstrated to significantly change the precision or position of paleomagnetic poles  
488 (Gerritsen et al., 2022), which is why we focused on maximizing the number of spot readings). This  
489 would leave only six datapoints; two from the Philippine Mobile Belt, with strongly varying  
490 declinations demonstrating that local block rotations must have occurred (e.g., Queaño et al., 2007,  
491 2009), and two from the North Maluku islands that are also in the deformed plate margin (e.g., Wu et  
492 al., 2016; Pubellier et al., 1991). Hence, the declinations of the PSP paleomagnetic database should  
493 not be used as basis for plate reconstructions.

494         This does not mean, of course, that paleomagnetic data exclude such rotations. It may well be  
495 that the entire PSP underwent regional vertical axis rotation. However, this rotation should follow  
496 from the kinematic reconstruction of the region and existing paleomagnetic data should not be used  
497 as input for such reconstructions. The paleomagnetic data obtained by Yamazaki et al. (2021) from  
498 oriented drill-cores from the PSP's interior may be the first declination data that are representative  
499 for a vertical-axis rotation of the entire PSP. These data suggest a ~50° clockwise rotation of the PSP  
500 since the mid-Oligocene (c. 28 Ma), which is distinctly less than the ~90° rotation that is  
501 incorporated in many PSP models. However, the small number of samples and the unknown  
502 uncertainty in declination, makes the data insufficient as a basis for kinematic reconstruction.

503 Yamazaki et al. (2021)'s study, however, shows that the large paleomagnetic datasets from the drill  
504 cores of the plate interior may provide a promising avenue towards obtaining quantitative  
505 constraints on plate rotation, but it is currently unknown what the uncertainty associated with the  
506 core-rotation correction is, and how this propagates into the final declination estimate. However, the  
507 mostly sedimentary rocks from the drill cores need to be corrected for inclination shallowing  
508 correction before also the inclination data can also be used for plate reconstruction.

509 We may use the data from igneous rocks in our compilation to infer PSP's paleolatitudinal  
510 motion. To this end, we compare the net paleolatitudinal displacements of the sampling sites  
511 between their moment of formation and the present, in a 'Huatung Basin-fixed' frame. We chose the  
512 Huatung Basin because it is the oldest oceanic lithosphere of the PSP and therefore exists throughout  
513 the reconstructed period. We reconstructed opening of PSP's oceanic basins using the available  
514 magnetic anomaly data (Hilde and Lee, 1984; Deschamps and Lallemand, 2002; Yamazaki et al.,  
515 2003; Sdrolias et al., 2004), making a 'Philippine plate motion chain'. The root of this plate motion  
516 chain is the Huatung Basin, and all motions are reconstructed relative to this microplate. We  
517 subsequently infer the paleolatitudinal correction that the Huatung Basin needs to get to fit with the  
518 paleomagnetic data in our compilation. The paleolatitude results show that a northward motion of  
519 about 15° since 45 Ma (Fig. 8) is suggested by the paleolatitude data, although the scatter is quite  
520 large. Our ~15° estimate is ~5° less northward motion than previous estimates (Louden, 1977;  
521 Kinoshita, 1980; Hall et al., 1995b; Haston and Fuller, 1991; Queaño et al., 2007, Yamazaki et al.,  
522 2010). The c. 5° difference may be explained by the fact that most boreholes are from the northern  
523 half of the PSP (Fig. 1), which underwent additional northward motion accommodated by spreading  
524 in the West Philippine Basin (Hilde and Lee, 1984). Without correction for the opening of the West  
525 Philippine Basin, a larger northward motion of up to 7° of the entire plate would be inferred. We find  
526 no systematic trend between paleolatitudinal mismatches and sampling location that would  
527 demonstrate a whole-plate vertical axis rotation. The single mid-Cretaceous pole obtained from the  
528 Philippine Mobile Belt (Balmater et al., 2015) suggests that the latitudinal position of the 'proto-PSP'  
529 at that time was about 10° south of its mid-Eocene position (Table 2), although more paleomagnetic  
530 data is needed to confidently determine the pre-Eocene latitudinal evolution of the proto-PSP. This  
531 single pole, however, suggests that the Philippine arcs cannot have been part of the Izanagi Plate,  
532 which was moving considerably faster to the north (Seton et al., 2012; Boschman et al., 2021; Wu et  
533 al., 2022). Instead, the proto-PSP formed part of a plate that was located in the junction region  
534 between the Tethyan and Panthalassa realms.

535 Finally, improved constraints on PSP motion may be obtained from the available drill-cores  
536 of the PSP, especially magnetostratigraphic data that contain large sample sets. These data are  
537 currently only useful for assessing general trends in paleolatitude evolution, but future efforts to  
538 correct for inclination shallowing may significantly improve their value. Subsequently, if the  
539 paleolatitude of different drill-cores is well-constrained, vertical-axis rotations may be deduced from  
540 well-dated paleolatitude-only data of drill locations spread throughout the plate.



541

542 **Figure 8:** Graph showing the change in latitude versus age, showing a more southerly position  
 543 (negative latitudes) of the PSP back in time. The data is plotted in a 'Huatung Basin reference frame' to  
 544 correct for intra-PSP plate motions (see main text). Paleolatitudes are colored by general sampling  
 545 location.

546

## 547 7. Conclusions

548 We reported new paleomagnetic data from Eocene, Oligocene and Miocene rocks from the island of  
 549 Guam, located in the forearc region of the Izu-Bonin-Mariana subduction zone. These data include  
 550 two Eocene poles that demonstrate rotation differences on Guam of as much as 35°, revealing that  
 551 local rotations related to forearc deformation likely occurred. We include our new data into a  
 552 compilation of previously published paleomagnetic data from the Philippine Sea Plate. Based on our  
 553 paleomagnetic results and a critical re-evaluation of existing data we conclude that:

- 554 1) It cannot be established to which extent paleomagnetic declinations from the Philippine  
 555 Mobile Belt, the northern Maluku Islands, and the Izu-Bonin-Marianas forearc provide  
 556 evidence of plate-wide rotation. Regional rotations demonstrably play a role, and  
 557 unequivocally robust data from the plate interior are currently not available.
- 558 2) The inclination-only data from igneous rocks are satisfied by a reconstruction in which all  
 559 microplates of the Philippine Sea Plate are reconstructed relative to the Huatung Basin, and  
 560 the for the latter a c. 15° northward motion since the mid-Eocene is reconstructed.

- 561 3) Drill-core paleomagnetic data with large sample sets from the stable plate interior are  
562 promising for future efforts to constrain the motion history of the Philippine Sea Plate.  
563 However, inclination shallowing should be corrected for, and uncertainties with for instance  
564 using the present-day field to correct for drill core rotation should be propagated into the  
565 analysis.
- 566 4) The paleomagnetic database does not require vertical axis rotations but does not preclude  
567 them.
- 568 5) Kinematic reconstructions of the Philippine Sea Plate should, for now, develop from  
569 systematic restorations of the geological records accreted at plate boundaries.

570

### 571 **Acknowledgements**

572 SHAvdL and DJJvH were funded by NWO Vici grant 865.17.001 to DJJvH. DPG is funded by a 'Ramón y  
573 Cajal' Fellowship (RYC2019-028244-I) and the grant KiTSuNE (PID2021-128801NA-I00) both  
574 funded by 'MCIN/AEI/ESF Investing in your future'. We thank Fagan Matthys and CJ Paulino for their  
575 help in the field.

576

### 577 **References**

- 578 Aurelio, M. A., Barrier, E., Rangin, C., & Müller, C. (1991). The Philippine Fault in the late Cenozoic  
579 tectonic evolution of the Bondoc-Masbate-N. Leyte area, central Philippines. *Journal of*  
580 *Southeast Asian Earth Sciences*, 6(3-4), 221-238.
- 581 Balmater, H. G., Manalo, P. C., Faustino-Eslava, D. V., Queaño, K. L., Dimalanta, C. B., Guotana, J. M. R.,  
582 Ramos, N. T., Payot, B. D., & Yumul Jr, G. P. (2015). Paleomagnetism of the Samar Ophiolite:  
583 Implications for the Cretaceous sub-equatorial position of the Philippine island  
584 arc. *Tectonophysics*, 664, 214-224.
- 585 Bird, P. (2003). An updated digital model of plate boundaries. *Geochemistry, Geophysics,*  
586 *Geosystems*, 4(3).
- 587 Bleil, U. (1982). Paleomagnetism of Deep Sea Drilling Project Leg 60 Sediments and Igneous Rocks  
588 from the Mariana Region. *Deep Sea Drill. Proj.* 60, 855-873.
- 589 Boschman, L. M., Van Hinsbergen, D. J., Langereis, C. G., Flores, K. E., Kamp, P. J., Kimbrough, D. L., ... &  
590 Spakman, W. (2021). Reconstructing lost plates of the Panthalassa Ocean through  
591 paleomagnetic data from circum-Pacific accretionary orogens. *American Journal of*  
592 *Science*, 321(6), 907-954.
- 593 Dankers, P. H. M., & Zijdeveld, J. D. A. (1981). Alternating field demagnetization of rocks, and the  
594 problem of gyromagnetic remanence. *Earth and Planetary Science Letters*, 53(1), 89-92.
- 595 Deenen, M. H., Langereis, C. G., van Hinsbergen, D. J., & Biggin, A. J. (2011). Geomagnetic secular  
596 variation and the statistics of palaeomagnetic directions. *Geophysical Journal*  
597 *International*, 186(2), 509-520.
- 598 Deschamps, A., & Lallemand, S. (2002). The West Philippine Basin: An Eocene to early Oligocene back  
599 arc basin opened between two opposed subduction zones. *Journal of Geophysical Research:*  
600 *Solid Earth*, 107(B12), EPM-1.
- 601 Dimalanta, C. B., Faustino-Eslava, D. V., Gabo-Ratio, J. A. S., Marquez, E. J., Padrones, J. T., Payot, B. D., ...  
602 & Yumul Jr, G. P. (2020). Characterization of the proto-Philippine Sea Plate: Evidence from the  
603 emplaced oceanic lithospheric fragments along eastern Philippines. *Geoscience*  
604 *Frontiers*, 11(1), 3-21.
- 605 Fisher, R. A. (1953). Dispersion on a sphere. *Proceedings of the Royal Society of London. Series A.*  
606 *Mathematical and Physical Sciences*, 217(1130), 295-305.
- 607 Fuller, M., Haston, R., & Almasco, J. (1989). Paleomagnetism of the Zambales ophiolite, Luzon,  
608 northern Philippines. *Tectonophysics*, 168(1-3), 171-203.



- 609 Gaina, C., & Müller, D. (2007). Cenozoic tectonic and depth/age evolution of the Indonesian gateway  
610 and associated back-arc basins. *Earth-Science Reviews*, 83(3-4), 177-203.
- 611 Gerritsen, D., Vaes, B., & van Hinsbergen, D. J. (2022). Influence of data filters on the position and  
612 precision of paleomagnetic poles: what is the optimal sampling strategy?. *Geochemistry,*  
613 *Geophysics, Geosystems*, 23(4), e2021GC010269.
- 614 Grommé, C. S., Wright, T. L., & Peck, D. L. (1969). Magnetic properties and oxidation of iron-titanium  
615 oxide minerals in Alae and Makaopuhi lava lakes, Hawaii. *Journal of Geophysical*  
616 *Research*, 74(22), 5277-5293.
- 617 Hall, R. (2002). Cenozoic geological and plate tectonic evolution of SE Asia and the SW Pacific:  
618 computer-based reconstructions, model and animations. *Journal of Asian earth sciences*, 20(4),  
619 353-431.
- 620 Hall, R., Ali, J. R., Anderson, C. D., & Baker, S. J. (1995a). Origin and motion history of the Philippine  
621 Sea Plate. *Tectonophysics*, 251(1-4), 229-250.
- 622 Hall, R., Fuller, M., Ali, J. R., & Anderson, C. D. (1995b). The Philippine Sea plate: magnetism and  
623 reconstructions. *Active margins and marginal basins of the Western Pacific*, 88, 371-404.
- 624 Haston, R. B., & Fuller, M. (1991). Paleomagnetic data from the Philippine Sea plate and their tectonic  
625 significance. *Journal of Geophysical Research: Solid Earth*, 96(B4), 6073-6098.
- 626 Haston, R. B., Stokking, L. B., & Ali, J. (1992). 31. Paleomagnetic data from holes 782A, 784A, and  
627 786A, Leg 125. *Proceedings of Ocean Drilling Program, Scientific Results (125)*, 535-545.
- 628 Haston, R., Fuller, M., & Schmidtke, E. (1988). Paleomagnetic results from Palau, West Caroline  
629 Islands: a constraint on Philippine Sea plate motion. *Geology*, 16(7), 654-657.
- 630 Hickey-Vargas, R., Ishizuka, O., & Bizimis, M. (2013). Age and geochemistry of volcanic clasts from  
631 DSDP Site 445, Daito Ridge and relationship to Minami-Daito Basin and early Izu-Bonin arc  
632 magmatism. *Journal of Asian Earth Sciences*, 70, 193-208.
- 633 Hickey-Vargas, R., Yogodzinski, G. M., Ishizuka, O., McCarthy, A., Bizimis, M., Kusano, Y., ... & Arculus, R.  
634 (2018). Origin of depleted basalts during subduction initiation and early development of the  
635 Izu-Bonin-Mariana island arc: Evidence from IODP expedition 351 site U1438, Amami-  
636 Sankaku basin. *Geochimica et Cosmochimica Acta*, 229, 85-111.
- 637 Hickey-Vargas, R. (1998). Origin of the Indian Ocean-type isotopic signature in basalts from  
638 Philippine Sea plate spreading centers: An assessment of local versus large-scale  
639 processes. *Journal of Geophysical Research: Solid Earth*, 103(B9), 20963-20979.
- 640 Hickey-Vargas, R. (2005). Basalt and tonalite from the Amami Plateau, northern West Philippine  
641 Basin: New Early Cretaceous ages and geochemical results, and their petrologic and tectonic  
642 implications. *Island Arc*, 14(4), 653-665.
- 643 Hilde, T. W., & Chao-Shing, L. (1984). Origin and evolution of the West Philippine Basin: a new  
644 interpretation. *Tectonophysics*, 102(1-4), 85-104.
- 645 Ishizuka, O., Hickey-Vargas, R., Arculus, R. J., Yogodzinski, G. M., Savov, I. P., Kusano, Y., ... & Sudo, M.  
646 (2018). Age of Izu-Bonin-Mariana arc basement. *Earth and Planetary Science Letters*, 481, 80-  
647 90.
- 648 Ishizuka, O., Tani, K., Reagan, M. K., Kanayama, K., Umino, S., Harigane, Y., ... & Dunkley, D. J. (2011a).  
649 The timescales of subduction initiation and subsequent evolution of an oceanic island  
650 arc. *Earth and Planetary Science Letters*, 306(3-4), 229-240.
- 651 Ishizuka, O., Tani, K., Taylor, R. N., Umino, S., Sakamoto, I., Yokoyama, Y., ... & Sekimoto, S. (2022).  
652 Origin and age of magmatism in the northern Philippine Sea basins. *Geochemistry, Geophysics,*  
653 *Geosystems*, 23(4).
- 654 Ishizuka, O., Taylor, R. N., Ohara, Y., & Yuasa, M. (2013). Upwelling, rifting, and age-progressive  
655 magmatism from the Oki-Daito mantle plume. *Geology*, 41(9), 1011-1014.
- 656 Ishizuka, O., Taylor, R. N., Yuasa, M., & Ohara, Y. (2011b). Making and breaking an island arc: A new  
657 perspective from the Oligocene Kyushu-Palau arc, Philippine Sea. *Geochemistry, Geophysics,*  
658 *Geosystems*, 12(5).
- 659 Ishizuka, O., Yuasa, M., Tamura, Y., Shukuno, H., Stern, R. J., Naka, J., ... & Taylor, R. N. (2010). Migrating  
660 shoshonitic magmatism tracks Izu-Bonin-Mariana intra-oceanic arc rift propagation. *Earth*  
661 *and Planetary Science Letters*, 294(1-2), 111-122.
- 662 Jarboe, N. A., Koppers, A. A., Tauxe, L., Minnett, R., & Constable, C. (2012, December). The online  
663 MagIC Database: data archiving, compilation, and visualization for the geomagnetic,

- 664 paleomagnetic and rock magnetic communities. In *Agu fall meeting abstracts* (Vol. 2012, pp.  
665 GP31A-1063).
- 666 Keating, B. (1980). Paleomagnetic study of sediments from deep sea drilling project leg 59. *Kroenke,*  
667 *L., Scott, R., et al., Init. Repts. DSDP, 59, 523-532.*
- 668 Keating, B. H., & Helsley, C. E. (1985). Implications of island arc rotations to the studies of marginal  
669 terranes. *Journal of geodynamics, 2*(2-3), 159-181.
- 670 Keating, B. H., & Herrero, E. (1980). Palcomagnetic studies of basalts and andesites from DSDP Leg  
671 59, Initial Rep. *Deep Sea Drill. Proj, 59, 533-544.*
- 672 Kinoshita, H. (1980). Paleomagnetism of sediment cores from Deep Sea Drilling Project Leg 58,  
673 Philippine Sea. *Init. Rept., DSDP, 58, 765-768.*
- 674 Kirschvink, J. (1980). The least-squares line and plane and the analysis of palaeomagnetic  
675 data. *Geophysical Journal International, 62*(3), 699-718.
- 676 Koymans, M. R., Langereis, C. G., Pastor-Galán, D., & van Hinsbergen, D. J. (2016). Paleomagnetism.  
677 org: An online multi-platform open source environment for paleomagnetic data analysis.  
678 *Computers and Geosciences, 93, 127-137.*
- 679 Koymans, M. R., van Hinsbergen, D. J. J., Pastor-Galán, D., Vaes, B., & Langereis, C. G. (2020). Towards  
680 FAIR paleomagnetic data management through Paleomagnetism. org 2.0. *Geochemistry,*  
681 *Geophysics, Geosystems, 21*(2), e2019GC008838.
- 682 Liu, J., Li, S., Cao, X., Dong, H., Suo, Y., Jiang, Z., ... & Foulger, G. R. (2023). Back-Arc Tectonics and Plate  
683 Reconstruction of the Philippine Sea-South China Sea Region Since the Eocene. *Geophysical*  
684 *Research Letters, 50*(5), e2022GL102154.
- 685 Liu, W., Gai, C., Feng, W., Cao, W., Guo, L., Zhong, Y., ... & Liu, Q. (2021). Coeval evolution of the eastern  
686 Philippine Sea Plate and the South China Sea in the Early Miocene: paleomagnetic and  
687 provenance constraints from ODP site 1177. *Geophysical Research Letters, 48*(14),  
688 e2021GL093916.
- 689 Louden, K. E. (1977). Paleomagnetism of DSDP sediments, phase shifting of magnetic anomalies, and  
690 rotations of the West Philippine Basin. *Journal of Geophysical Research, 82*(20), 2989-3002.
- 691 McCabe, R., & Uyeda, S. (1983). Hypothetical model for the bending of the Mariana Arc. *Washington*  
692 *DC American Geophysical Union Geophysical Monograph Series, 27, 281-293.*
- 693 McFadden, P. L., & McElhinny, M. W. (1988). The combined analysis of remagnetization circles and  
694 direct observations in palaeomagnetism. *Earth and Planetary Science Letters, 87*(1-2), 161-  
695 172.
- 696 Meert, J. G., Pivarunas, A. F., Evans, D. A., Pisarevsky, S. A., Pesonen, L. J., Li, Z. X., ... & Salminen, J. M.  
697 (2020). The magnificent seven: a proposal for modest revision of the quality  
698 index. *Tectonophysics, 790, 228549.*
- 699 Meijer, A., Reagan, M., Ellis, H., Shafiqullah, M., Sutter, J., Damon, P., & Kling, S. (1983). Chronology of  
700 volcanic events in the eastern Philippine Sea. *Washington DC American Geophysical Union*  
701 *Geophysical Monograph Series, 27, 349-359.*
- 702 Morishita, T., Tani, K. I., Soda, Y., Tamura, A., Mizukami, T., & Ghosh, B. (2018). The uppermost mantle  
703 section below a remnant proto-Philippine Sea island arc: Insights from the peridotite  
704 fragments from the Daito Ridge. *American Mineralogist: Journal of Earth and Planetary*  
705 *Materials, 103*(7), 1151-1160.
- 706 Mullender, T. A. T., Van Velzen, A. J., & Dekkers, M. J. (1993). Continuous drift correction and separate  
707 identification of ferrimagnetic and paramagnetic contributions in thermomagnetic  
708 runs. *Geophysical Journal International, 114*(3), 663-672.
- 709 Mullender, T. A., Frederichs, T., Hilgenfeldt, C., de Groot, L. V., Fabian, K., & Dekkers, M. J. (2016).  
710 Automated paleomagnetic and rock magnetic data acquisition with an in-line horizontal “2 G”  
711 system. *Geochemistry, Geophysics, Geosystems, 17*(9), 3546-3559.
- 712 NOAA National Centers for Environmental Information. 2022: ETOPO 2022 15 Arc-Second Global  
713 Relief Model. NOAA National Centers for Environmental Information.
- 714 Pubellier, M., Bader, A. G., Rangin, C., Deffontaines, B., & Quebral, R. (1999). Upper plate deformation  
715 induced by subduction of a volcanic arc: the Snellius Plateau (Molucca Sea, Indonesia and  
716 Mindanao, Philippines). *Tectonophysics, 304*(4), 345-368.
- 717 Queaño, K. L., Ali, J. R., Milsom, J., Aitchison, J. C., & Pubellier, M. (2007). North Luzon and the  
718 Philippine Sea Plate motion model: Insights following paleomagnetic, structural, and age-  
719 dating investigations. *Journal of Geophysical Research: Solid Earth, 112*(B5).

- 720 Queaño, K. L., Ali, J. R., Pubellier, M., Yumul Jr, G. P., & Dimalanta, C. B. (2009). Reconstructing the  
721 Mesozoic-early Cenozoic evolution of northern Philippines: Clues from palaeomagnetic studies  
722 on the ophiolitic basement of the Central Cordillera. *Geophysical Journal International*, 178(3),  
723 1317-1326.
- 724 Reagan, M. K., & Meijer, A. (1984). Geology and geochemistry of early arc-volcanic rocks from  
725 Guam. *Geological Society of America Bulletin*, 95(6), 701-713.
- 726 Reagan, M. K., Heaton, D. E., Schmitz, M. D., Pearce, J. A., Shervais, J. W., & Koppers, A. A. (2019).  
727 Forearc ages reveal extensive short-lived and rapid seafloor spreading following subduction  
728 initiation. *Earth and Planetary Science Letters*, 506, 520-529.
- 729 Reagan, M. K., Ishizuka, O., Stern, R. J., Kelley, K. A., Ohara, Y., Blichert-Toft, J., ... & Woods, M. (2010).  
730 Fore-arc basalts and subduction initiation in the Izu-Bonin-Mariana system. *Geochemistry,*  
731 *Geophysics, Geosystems*, 11(3).
- 732 Reagan, M. K., McClelland, W. C., Girard, G., Goff, K. R., Peate, D. W., Ohara, Y., & Stern, R. J. (2013). The  
733 geology of the southern Mariana fore-arc crust: Implications for the scale of Eocene volcanism  
734 in the western Pacific. *Earth and Planetary Science Letters*, 380, 41-51.
- 735 Richter, C., & Ali, J. R. (2015). Philippine sea plate motion history: Eocene-Recent record from ODP  
736 Site 1201, central West Philippine basin. *Earth and Planetary Science Letters*, 410, 165-173.
- 737 Sager, W. W., & Carvallo, C. (2022). Paleomagnetism and paleolatitude of igneous drill core samples  
738 from the Izu-Bonin forearc and implications for Philippine Sea plate  
739 motion. *Tectonophysics*, 841, 229573.
- 740 Sdrolias, M., Roest, W. R., & Müller, R. D. (2004). An expression of Philippine Sea plate rotation: the  
741 Parece Vela and Shikoku basins. *Tectonophysics*, 394(1-2), 69-86.
- 742 Seno, T., & Maruyama, S. (1984). Paleogeographic reconstruction and origin of the Philippine  
743 Sea. *Tectonophysics*, 102(1-4), 53-84.
- 744 Seton, M., Müller, R. D., Zahirovic, S., Gaina, C., Torsvik, T., Shephard, G., Talsma, A., Gurnis, M., Turner,  
745 M., Maus, S., & Chandler, M. (2012). Global continental and ocean basin reconstructions since  
746 200 Ma. *Earth-Science Reviews*, 113(3-4), 212-270.
- 747 Siegrist, H. G., Reagan, M. K., RH, R., & JW, J. (2008). Geologic Map and Sections of Guam. *Mariana*  
748 *Islands (1: 50,000), Revision of original map from USGS Professional Report A, 403*, 1964.
- 749 Tauxe, L. (2010). *Essentials of paleomagnetism*. Univ of California Press.
- 750 Tauxe, L., & Kent, D. V. (2004). A simplified statistical model for the geomagnetic field and the  
751 detection of shallow bias in paleomagnetic inclinations: was the ancient magnetic field  
752 dipolar?. *Geophysical Monograph Series*, 145, 101-115.
- 753 Tracey Jr, J. I., Schlanger, S. O., Stark, J. T., Doan, D. B., & May, H. G. (1964). *General geology of*  
754 *Guam* (No. 403-A).
- 755 Vaes, B., Gallo, L. C., & van Hinsbergen, D. J. (2022). On pole position: causes of dispersion of the  
756 paleomagnetic poles behind apparent polar wander paths. *Journal of Geophysical Research:*  
757 *Solid Earth*, 127(4), e2022JB023953.
- 758 Vaes, B., Li, S., Langereis, C. G., & van Hinsbergen, D. J. (2021). Reliability of palaeomagnetic poles  
759 from sedimentary rocks. *Geophysical Journal International*, 225(2), 1281-1303.
- 760 Van Hinsbergen, D. J. J., Dekkers, M. J., Bozkurt, E., & Koopman, M. (2010). Exhumation with a twist:  
761 Paleomagnetic constraints on the evolution of the Menderes metamorphic core complex,  
762 western Turkey. *Tectonics*, 29(3).
- 763 Wu, J., Lin, Y. A., Flament, N., Wu, J. T. J., & Liu, Y. (2022). Northwest Pacific-Izanagi plate tectonics  
764 since Cretaceous times from western Pacific mantle structure. *Earth and Planetary Science*  
765 *Letters*, 583, 117445.
- 766 Wu, J., Suppe, J., Lu, R., & Kanda, R. (2016). Philippine Sea and East Asian plate tectonics since 52 Ma  
767 constrained by new subducted slab reconstruction methods. *Journal of Geophysical Research:*  
768 *Solid Earth*, 121(6), 4670-4741.
- 769 Xu, J., Ben-Avraham, Z., Kelty, T., & Yu, H. S. (2014). Origin of marginal basins of the NW Pacific and  
770 their plate tectonic reconstructions. *Earth-Science Reviews*, 130, 154-196.
- 771 Yamazaki, T., Chiyonobu, S., Ishizuka, O., Tajima, F., Uto, N., & Takagawa, S. (2021). Rotation of the  
772 Philippine Sea plate inferred from paleomagnetism of oriented cores taken with an ROV-based  
773 coring apparatus. *Earth, Planets and Space*, 73(1), 1-10.

- 774 Yamazaki, T., Seama, N., Okino, K., Kitada, K., Joshima, M., Oda, H., & Naka, J. (2003). Spreading  
775 process of the northern Mariana Trough: Rifting-spreading transition at 22 N. *Geochemistry,*  
776 *Geophysics, Geosystems, 4*(9).
- 777 Yamazaki, T., Takahashi, M., Iryu, Y., Sato, T., Oda, M., Takayanagi, H., Chiyonobu, S., Nishimura, A.,  
778 Nakazawa, T., & Ooka, T. (2010). Philippine Sea Plate motion since the Eocene estimated from  
779 paleomagnetism of seafloor drill cores and gravity cores. *Earth, Planets and Space, 62*(6), 495-  
780 502.
- 781 Yumul Jr, G. P., Dimalanta, C. B., Gabo-Ratio, J. A. S., Queaño, K. L., Armada, L. T., Padrones, J. T., ... &  
782 Marquez, E. J. (2020). Mesozoic rock suites along western Philippines: Exposed proto-South  
783 China Sea fragments?. *Journal of Asian Earth Sciences: X, 4*, 100031.
- 784 Zahirovic, S., Seton, M., & Müller, R. D. (2014). The cretaceous and cenozoic tectonic evolution of  
785 Southeast Asia. *Solid Earth, 5*(1), 227-273.
- 786 Zijdeveld, J. D. A. (1967). The natural remanent magnetizations of the Exeter volcanic traps  
787 (Permian, Europe). *Tectonophysics, 4*(2), 121-153.